MSH3 Promotes Dynamic Behavior of Trinucleotide Repeat Tracts *In Vivo*

Gregory M. Williams* and Jennifer A. Surtees*,†,1

*Department of Biochemistry and †Genetics, Genomics and Bioinformatics Program, School of Medicine and Biomedical Sciences, State University of New York at Buffalo, New York 14214

ORCID ID: 0000-0003-4243-0933 (J.A.S.)

ABSTRACT Trinucleotide repeat (TNR) expansions are the underlying cause of more than 40 neurodegenerative and neuromuscular diseases, including myotonic dystrophy and Huntington's disease, yet the pathway to expansion remains poorly understood. An important step in expansion is the shift from a stable TNR sequence to an unstable, expanding tract, which is thought to occur once a TNR attains a threshold length. Modeling of human data has indicated that TNR tracts are increasingly likely to expand as they increase in size and to do so in increments that are smaller than the repeat itself, but this has not been tested experimentally. Genetic work has implicated the mismatch repair factor *MSH3* in promoting expansions. Using *Saccharomyces cerevisiae* as a model for *CAG* and *CTG* tract dynamics, we examined individual threshold-length TNR tracts *in vivo* over time in *MSH3* and *msh3Δ* backgrounds. We demonstrate, for the first time, that these TNR tracts are highly dynamic. Furthermore, we establish that once such a tract has expanded by even a few repeat units, it is significantly more likely to expand again. Finally, we show that threshold- length TNR sequences readily accumulate net incremental expansions over time through a series of small expansion and contraction events. Importantly, the tracts were substantially stabilized in the *msh3Δ* background, with a bias toward contractions, indicating that Msh2-Msh3 plays an important role in shifting the expansion-contraction equilibrium toward expansion in the early stages of TNR tract expansion.

KEYWORDS *Saccharomyces cerevisiae*; Msh2-Msh3; mismatch repair; trinucleotide repeat tract

THE EXPANSION of trinucleotide repeat (TNR) sequences is the underlying cause of over 40 neurodegenerative and neuromuscular diseases (Castel *et al.* 2010; McMurray 2010). TNR sequences made of $(CNG)_n$ repeats are of particular interest because of their role in causing Huntington's disease (HD) and myotonic dystrophy type 1 (DM1), as well as a number of other diseases (McMurray 2010). TNR tracts within the normal range (which is tract dependent) are stably maintained within that range (Figure 1). However, through a mechanism(s) that remains unclear, a TNR tract can expand, increasing the number of repeats within the tract. Initially, this brings the tract into a threshold-length range (Gannon *et al.* 2012; Concannon and Lahue 2014) (Figure 1 and Figure 2), in which these somewhat longer tracts are not pathogenic but are increasingly susceptible to expansion; individuals with this phenomenon are carriers for disease. Once a tract has expanded sufficiently, it crosses a threshold; tracts above this threshold (which is disease specific) are pathogenic and cause disease (Figure 1). As the size of the tract increases, it becomes increasingly unstable and prone to changes in length, particularly expansions.

The dynamic behavior of TNR tracts that are *within* the threshold range (*i.e.*, more susceptible to expansions) and the manner in which they occur *in vivo* remain unclear. Studies of TNR tract length changes have largely relied on end point experiments and therefore do not address the dynamic behavior of the tracts, *i.e.*, the rate at which tracts continue to expand. Modeling of human data has predicted that threshold-length TNR tracts will continue to increase in length in increments smaller than the repeat itself (Higham *et al.* 2012; Morales *et al.* 2012; Higham and Monckton 2013), although this has never been demonstrated directly. Single-sperm typing studies in humans demonstrated small expansion and contraction events (one–two repeats) in TNR

doi: 10.1534/genetics.115.177303
Manuscript received April 13, 2015; accepted for publication May 4, 2015; published Early Online May 11, 2015.
Supporting information is available online at www.genetics.org/lookup/suppl/doi:10.1534/genetics.115.177303/-/DC1
[1]Corresponding author: Department of Biochemistry, State University of New York at Buffalo, 619 Biomedical Research Building, 3435 Main Street, Buffalo, NY 14214. E-mail: jsurtees@buffalo.edu

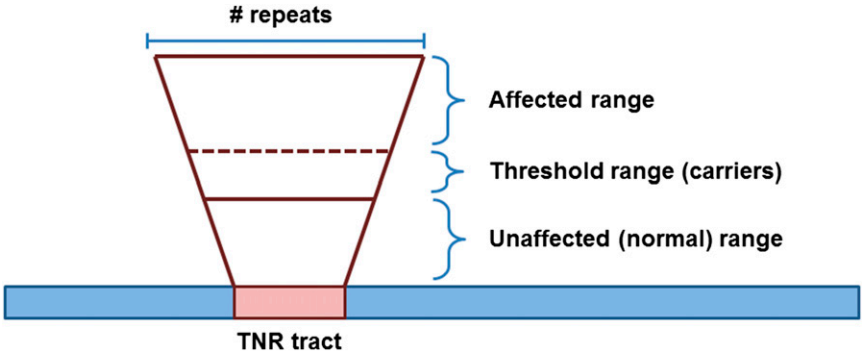

Figure 1 Size of trinucleotide repeat (TNR) tract determines disease phenotype. The normal range of a TNR tract is present in unaffected individuals. This range varies depending on the TNR sequence and position with respect to the relevant gene. As the TNR tract gets larger, it enters the threshold or premutation range. These individuals are typically unaffected by disease but are carriers because these somewhat larger tracts are prone to further expansion. Once the TNR tract expands into the affected range, individuals are symptomatic and are affected by disease.

sequences in Kennedy's disease, HD, and DM1 patients (Zhang *et al.* 1994; Leeflang *et al.* 1995, 1999; Martorell *et al.* 2004), particularly in alleles near the pathogenic threshold (Zhang *et al.* 1994; Leeflang *et al.* 1995; Castel *et al.* 2010). These observations are consistent with the existence of an equilibrium between expansion and contraction events. As the tract length increased in sperm cells, there was significant bias toward expansions *vs.* contractions. The sizes of the observed expansion and contraction events were similar to our *in vitro* observations (one–two repeats) (Kantartzis *et al.* 2012), in contrast to larger expansion events observed in nondividing cells or postmitotic neurons (McMurray 2010).

One factor known to contribute to $(CNG)_n$ tract expansions is the mismatch repair (MMR) complex Msh2-Msh3 (MutSβ in mammals). Typically, Msh2-Msh3 recognizes and binds insertion-deletion loops (IDLs) that result from DNA polymerase slippage events, often within repetitive sequences (Lovett 2004; Li 2008). These are then targeted for excision and resynthesis. Strikingly, rather than correcting them, Msh2-Msh3 promotes TNR expansions in both mammalian somatic and germ cells (Castel *et al.* 2010; McMurray 2010). This difference is likely related to the propensity of $(CNG)_n$ sequences to form secondary structures once they have slipped and are single stranded owing to the inherent complementarity of the C's and G's within the repeat sequence (Castel *et al.* 2010; McMurray 2010) and to the manner in which Msh2-Msh3 interacts with these unique structures (Lang *et al.* 2011). As the tract length increases, the potential complexity of the secondary structure increases (Gacy and McMurray 1998; Pearson and Sinden 1998; Slean *et al.* 2013). Nonetheless, loss of *MSH2* or *MSH3* leads to a significant decrease in expansion events in mouse models of HD (Manley *et al.* 1999; Owen *et al.* 2005) and MD1 (van den Broek *et al.* 2002; Foiry *et al.* 2006). Similarly, Msh3 promotes expansions in human cells (Gannon *et al.* 2012; Halabi *et al.* 2012). We recently demonstrated a significant decrease in expansion of both *CAG* and *CTG* repeat tracts in *Saccharomyces cerevisiae* in an *msh3Δ* background (Kantartzis *et al.* 2012).

The role that Msh2-Msh3 plays in promoting TNR expansions remains unclear. Our *in vitro* results indicate that yeast Msh2-Msh3 interferes with proper Okazaki fragment processing by Rad27 (Fen1) and Cdc9 (Lig1) in the presence of a dynamic *CTG* or *CAG* repeat tract, leading to small incremental expansions and providing mechanistic insight into the role of Msh2-Msh3 in replication-dependent TNR expansions (Kantartzis *et al.* 2012). This model predicts that Msh2-Msh3 modulates TNR dynamics *in vivo*. Subsequently, Stevens *et al.* (2013) demonstrated that Msh2-Msh3 can promote expansions *in vitro* using human cell culture extracts in a replication-independent manner, consistent with a role for Msh2-Msh3 in promoting expansions in somatic as well as germline cells (Castel *et al.* 2010; McMurray 2010).

To address the question of threshold-length tract behavior and the role that *MSH3* plays in that behavior, we have established *S. cerevisiae* as a model to visualize and characterize individual tract dynamics in dividing cells as a function of time through multiple generations. We observed highly dynamic DNA sequences with progressive, incremental expansion in an *MSH3* background. The TNR tract dynamics were substantially altered in the absence of *MSH3*, resulting in more stable repeat sequences. These observations indicate that *MSH3* is an important factor in promoting the transition of a TNR tract into the pathogenic range.

Methods and Materials

Strains and media

All yeast transformations were performed using the lithium acetate method (Gietz *et al.* 1992). Yeast strains were derived from the S288c background and are detailed in Supporting Information, Table S1. In addition to the *msh3Δ*::*KANMX* strain, constructed by amplifying a chromosomal *msh3Δ*::*KANMX* fragment from the yeast deletion collection that was integrated into the *MSH3* chromosomal location in FY86 (Kantartzis *et al.* 2012), we constructed a second *msh3Δ* strain in FY86. The *msh3Δ*::*hisG* strain was constructed by integration of a *hisG-URA3-hisG* cassette into the *MSH3* locus using pEAI88 (Lyndaker *et al.* 2008). Integration was selected on synthetic medium lacking uracil. The *URA3* gene was selected against by growth on 5-FOA, which selects for recombination between the two *hisG* moieties (Alani *et al.* 1987), resulting in a single *hisG* interrupting the *MSH3* ORF. The tract dynamics in the two *msh3Δ* backgrounds were indistinguishable.

TNR substrates were integrated into *MSH3* and *msh3Δ* strains, as described previously (Miret *et al.* 1998; Dixon *et al.* 2004; Kantartzis *et al.* 2012). Briefly, each plasmid was

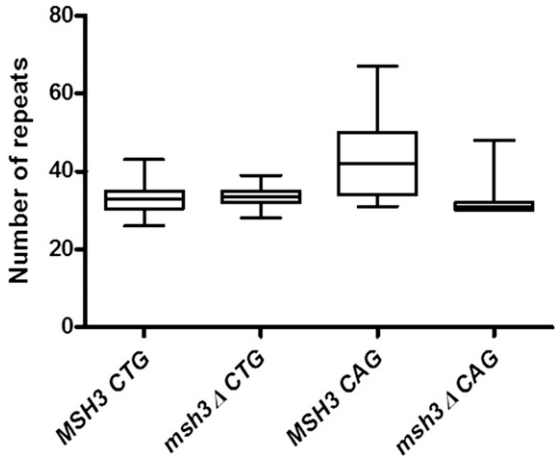

Figure 2 Distribution of tract size following initial expansion. Whisker plot of the median tract size following selection on 5-FOA plates in *MSH3* and *msh3Δ* strains. The $(CAG)_{25}$ and $(CTG)_{25}$ tracts were examined. The plot was created using GraphPad Prism. Both the median and mean sizes of the *CAG* tracts are statistically different from the *CTG* tracts (Wilcox rank, *t*-test, $P < 0.0001$). The median and mean *CAG* tract lengths in the *MSH3* background are statistically different from the *CAG* tract in the *msh3Δ* background, whereas the *CTG* tract size is similar in both strain backgrounds (Wilcox rank, *t*-test, $P < 0.0001$).

digested with *Bsu*36I and then transformed to allow integration by homologous recombination at the *LYS2* chromosomal locus. Integrants were selected on synthetic medium lacking histidine. Single integration of the TNR substrate at the correct location was confirmed by Southern blot, as described previously (Dixon *et al.* 2004). Three independent single integrants for each substrate were selected for further analysis. This was repeated in all three strain backgrounds. Prior to performing the expansion assay, each strain was struck out on synthetic medium lacking histidine and uracil to obtain single colonies. Individual colonies were analyzed by colony PCR to ensure that they contained the proper number of repeats (Dixon *et al.* 2004). A subset also was sequenced to confirm the tract using SO299 as a primer (5′-ACTTGGG GAGAGGTGCG) (Dixon *et al.* 2004; Kantartzis *et al.* 2012).

Growth curves

Saturated cultures were diluted 1:100 in synthetic medium lacking histidine. Absorbance (A_{600}) of the cultures was measured every 45 min for 10 hr. The cultures were allowed to saturate overnight and were then diluted again and the growth curve repeated. There was no difference in the growth curves of the different strains tested or between the first and second days of growth, with a doubling time of approximately 140 min once the cells reached exponential phase (Figure S1 and data not shown). In 24 hr, the cells underwent approximately six cell divisions. For microcolony growth curves, individual cells were tracked using a dissection microscope with a micromanipulator, with examination every 30 min for 10 hr. The daughter cells were removed from the mother following each cell division and placed elsewhere on the plate. There was no observable difference in the timing of the cell cycle between the *MSH3* and the *msh3Δ* strains, which both exhibited a doubling time of approximately 140 min. Generation times of growth in liquid and on solid medium were confirmed by counting the number of cells in culture and in colonies of different sizes using a hemacytometer.

Liquid time course protocol

Expanded *CAG* or *CTG* tracts in either the wild-type or *msh3Δ* background were selected by growth on SC medium lacking histidine (to maintain the tract construct) and containing 5-FOA (to select for expansions that abrogate *URA3* expression; United States Biological), as described previously (Miret *et al.* 1998; Kantartzis *et al.* 2012). The size of the tract was analyzed by colony PCR using SO295 and SO296 (Kantartzis *et al.* 2012). The PCR cycle consisted of one round at 95° for 5 min and then 35 cycles at 95° for 2 min, 53° for 1 min, and 72° for 1 min, followed by a final extension at 72° for 10 min. The PCR products were digested with *Sph*I and *Afl*II and then electrophoresed through a 12% polyacrylamide gel in 1× TBE buffer, and the gel was stained with ethidium bromide (EtBr, 0.5 μg/ml) to determine tract size. The gels were imaged on a GelDoc system (Bio-Rad) and quantified by ImageQuant (Molecular Dynamics).

Three independent colonies were selected for expansion events in each genetic background, *i.e.*, $(CTG)_{25}$ and $(CAG)_{25}$ tracts in *MSH3* and *msh3Δ* . Each colony was resuspended in 106 mL of SC medium lacking histidine (SC-his) and grown to saturation at 30° with shaking. Then 5 ml of each saturated culture was used to prepare genomic DNA (gDNA). From each saturated culture, a logarithmically growing (log-phase) culture and a stationary-phase culture were established. For the logarithmic culture, 10 ml of SC-his was inoculated with 200 μl of the saturated culture and grown at 30° in a shaker for 24 hr. This dilution was repeated every 24 hr for the duration of the time course. The remainder of each saturated culture was collected by centrifugation, and the pellet was washed twice with sterile water and then resuspended in 100 mL of sterile distilled water. These stationary-phase cultures were maintained at 30° in the shaker for the duration of the time course. The stationary-phase cell pellet was washed and resuspended in fresh distilled water every 48 hr.

Every 24 hr, 5 ml from each log- and stationary-phase culture was used to prepare gDNA. On days 1, 7, and 14, dilutions from each culture were plated on SC-his to get individual colonies. PCR was performed, as described earlier, to amplify the tract using the gDNA from each time point as a template. Colony PCR was performed on individual colonies from days 7 and 14.

PCR controls

PCR has been used extensively to examine TNR tract sizes (Zhang *et al.* 1994; Leeflang *et al.* 1995, 1999; Miret *et al.* 1998; Dixon *et al.* 2004). Nonetheless, we performed several controls to ensure that these observed expansions were not PCR artifacts. First, we performed PCR reactions using the *CAG* or *CTG* tract plasmid (used to integrate the tract into

the yeast chromosome) (Miret *et al.* 1998; Kantartzis *et al.* 2012) as a template alongside every set of PCR reactions. A subset of these reactions is shown in Figure S2 and clearly demonstrates the ability of *Taq* polymerase to accurately and reproducibly amplify a tract of 25 repeats. In over 100 PCR reactions using the plasmid as a template, the major product was a 75-base-pair fragment in every case. Minor products were observed occasionally at larger sizes and likely represent background due to polymerase error. Based on Southern blots of 20 independent plasmid amplification reactions, ≥85% (±1.5% SEM) of the total product is the 75-base-pair unexpanded tract (Figure S3, right, and data not shown). As an additional control, we performed five independent colony PCR reactions simultaneously from the same colony to assess reproducibility of *Taq* in amplifying both expanded and unexpanded tracts by colony PCR (Figure S4). The resulting pattern of PCR products was very consistent and reproducible.

Mixing experiment

To determine whether the ratio of PCR products was representative of the input DNA template, we performed PCR reactions that contained different ratios of genomic DNA from cells with either an unexpanded and an expanded TNR tract. The DNA was amplified and then quantified (Figure S5). gDNA was prepared from cells carrying an unexpanded tract and from cells carrying an expanded tract using standard techniques. The DNA concentration of each preparation was measured by NanoDrop (Thermo Scientific). The gDNA from both backgrounds was used as a template for PCR at different concentration ratios. Ratios of 1:1, 1:5, 1:10, and 1:20 unexpanded-expanded and expanded-unexpanded were tested as templates in the standard PCR reaction (described earlier).

The ratio of unexpanded product to expanded product correlated with the input DNA, although at a 1:1 ratio there was a notable bias toward amplification of the *unexpanded* tract. This reassured us that we were not preferentially amplifying the expanded products and thereby overestimating the expansion rate. Furthermore, the PCR output was a reasonable representation of the input template, and we are more likely to err on the side of underestimating expansion events when performing PCR with a nonhomogeneous template population. We do note that this may lead us to underestimate expansions in the *msh3Δ* background as well.

Colony PCR time course protocol

Expanded TNR tracts were selected, and the tract size was analyzed and measured, as described earlier. Tracts of different length were selected for this experiment. Colonies with expanded tracts were incubated continuously at 30° for 10–14 days . Colony PCR was performed every 24 hr and the tract analyzed by PCR and digestion. Colony PCR was performed either from the same side of the colony or from around the perimeter of the colony with similar results. When taken from around the colony, the samples were taken from four locations in rotations corresponding to 12, 3, 6, and 9 o'clock. Because the cells were always sampled from the perimeter of the colony, we assumed a generation time of ~140 min, as described earlier.

Microcolony PCR time course protocol

Expanded TNR tracts were selected, and the tract size was analyzed and measured, as described earlier. Colonies with expanded tracts were resuspended in sterile water. Each suspension was run in a line on an SC-his plate. Using a micromanipulator on a dissection microscope, three single cells from each suspension were selected for the time course. Each plate was incubated at 30° for 15–20 hr, until the microcolony contained between 250 and 1000 cells; this was the size necessary for reproducible PCR results. Three individual cells were removed from the microcolony to continue the time course. (Three cells were selected to ensure that at least one microcolony arose in the next round.) The remaining cells were used for colony PCR to assess the size of the TNR tract. The plate then was incubated at 30° for another 15–20 hr to allow growth of the four individual cells to a microcolony. One of the four cells was selected to propagate and continue the time course. The time course was continued through 14 cycles. At each step, tract sizes were analyzed by PCR, as described earlier. Time points in which no PCR amplification was observed were excluded from our analysis.

Southern blotting

To verify that the PCR products contained the TNR tract, Southern blots were performed (Sambrook and Russell 2001). Briefly, PCR reactions were electrophoresed through a 12% acrylamide gel (1× TBE). The gel was transferred to a nylon membrane, cross-linked and hybridized with a radiolabeled probe, as described previously (Dixon *et al.* 2004; Kantartzis *et al.* 2012). The probe was a PCR product amplified from pBL69 (Miret *et al.* 1998) with SO295 and SO296 and then digested with *Sph*I. The resulting fragment was radiolabeled using the Takara Random Priming Kit. The membrane was washed, dried, and exposed to a PhosphorImager screen and imaged and quantified, where applicable, in ImageQuant.

Mutation-rate calculations

To calculate the mutation rates, the probability of a change in tract size was treated as a binomial distribution with P = proportion of tracts with a change in length and q = proportion of tracts with no length change. The rate of tract change was defined as the number of changes observed per number of cells examined per generation. For the liquid time courses, the mutation rate was derived from the number of tract changes observed per colonies tested divided by 126 generations per culture. For the colony and microcolony time courses, the proportion of tract changes was calculated as the number of tract changes divided by the number time points examined divided by the number of generations from one time point to the next. Growth curve experiments in both liquid medium and on plates were used to determine the number of generations for these calculations (Figure S1 and data not shown). To

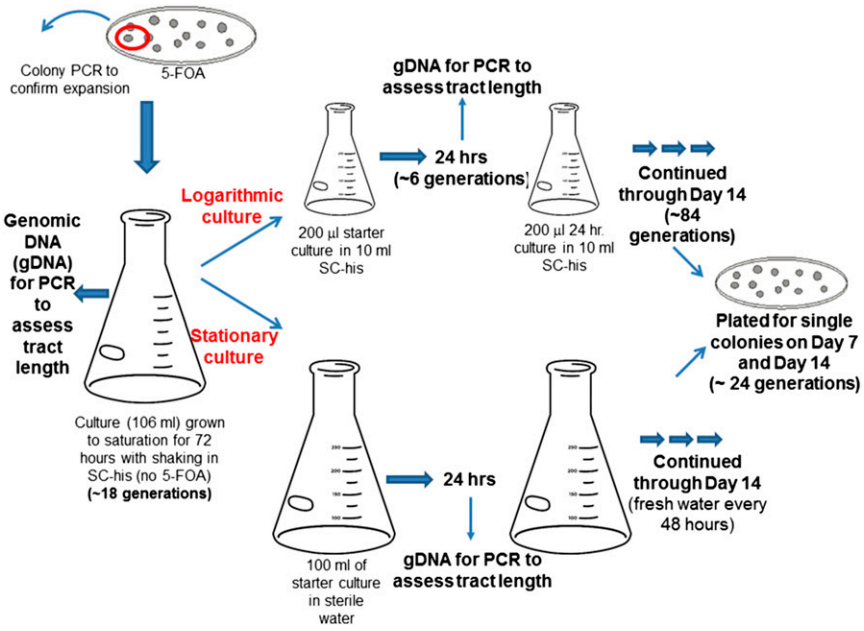

Figure 3 Schematic of the liquid time course experiment protocols. Individual colonies with TNR tract expansions were selected on plates containing 5-FOA; the tract increase was confirmed by colony PCR in each case. A single colony with an expanded tract was used to inoculate a large culture that was grown to saturation over 72 hr (~18 generations). From this population, genomic DNA (gDNA) was isolated. Then parallel log- and stationary-phase cultures were established (see *Materials and Methods*) and propagated for 14 days. gDNA was prepared from each culture every 24 hr (~6 generations) and then subjected to PCR to evaluate tract size. A sample from each log- and stationary-phase cultures was diluted and plated to isolate individual colonies (~26 generations), which then were subjected to PCR to assess tract length. This experiment is akin to a mutation-accumulation experiment, although we limited the number of cell divisions (~6 per time point) to mitigate any fitness effects of tract changes. This is an end point experiment that indicated that additional expansions are observable in a 2-week time span. Further, it allowed us to observe general trends in the population as well as looking at individual tract lengths from single colonies. See *Materials and Methods* for additional details.

calculate 95% confidence intervals (95% C.I.) on the mutation rates, the *F*-statistic was used (Zar 1999; Foster *et al.* 2006).

Plasmid retention assays

Three independent *MSH3* isolates with large tracts, ranging from 33 to 48 repeats, were transformed with a low-copy plasmid (*ARS CEN*) carrying the *KANMX* cassette, which confers resistance to G418 (Wach *et al.* 1994). Three independent *MSH3* isolates with small tracts, ranging from 25 to 30 repeats, were transformed with a low-copy plasmid (*ARS CEN*) carrying the *NATMX* cassette, which confers resistance to nourseothricin (Goldstein and McCusker 1999). The two plasmids had indistinguishable retention rates in the absence of selection (data not shown). In each of three cultures, one isolate with a large tract and one isolate with a small tract were mixed 1:1 and were taken through a time course in SC-his for 6 days (see the section *Liquid time course protocol* earlier) in the absence of selection for either plasmid. In the first set, a 40-repeat tract and a 25-repeat (unexpanded) tract were mixed. In the second set, a 38-repeat tract and a 31-repeat tract were mixed. In the third set, a 33-repeat tract and a 25-repeat tract were mixed. Every 24 hr, a sample of the culture was plated on SC-his medium. Each individual colony was tested for growth on YPD medium containing either G418 or nourseothricin. The percentages of cells retaining resistance for one drug or the other are plotted in Figure S6.

Results

The major goal of this study was to determine how a TNR tract behaves as it approaches a pathogenic length. To do this, we adapted the *in vivo URA3*-based reporter system in *S. cerevisiae* that we used previously (Miret *et al.* 1998; Kantartzis *et al.* 2012) and examined larger threshold-length $(CNG)_n$ tract dynamics over time in the presence and absence of *MSH3*. Previous work indicated that 25-repeat tracts approach the threshold length in this system (Miret *et al.* 1998; Concannon and Lahue 2014). Therefore, we started with $(CTG)_{25}$ and $(CAG)_{25}$ TNR tracts and selected single colonies with expanded tracts, as described previously (see *Materials and Methods*) (Miret *et al.* 1998; Kantartzis *et al.* 2012). We took this analysis further by determining (1) whether expanded tracts continue to expand, (2) at what rate tracts expand, and (3) in what increments expansions occur. Throughout this work we will follow the following convention: a *CTG* or *CAG* tract refers to the sequence of the *nascent* DNA on the lagging strand. Thus, a *CTG* tract refers to *CAG* on the template strand, and the newly replicated DNA will contain the *CTG* tract.

We took three different approaches to answering these questions using PCR techniques to monitor tract length. First, we performed liquid time course experiments to determine whether *additional expansions* accumulated in replicating cells within a reasonable time frame (Figure 3, Figure 4, and Figure 5). Once a tract has expanded, it is not possible to select for further expansions; this tested the feasibility of our approach. Second, we sought to observe dynamic tract size changes in a single colony over time (Figure 6, Figure 7, Figure 8, and Figure 9). The expanded tract of an individual growing colony was monitored through multiple generations in the absence of selection. Third, we isolated individual cells from colonies with expanded tracts and monitored tract dynamics over a well-defined number

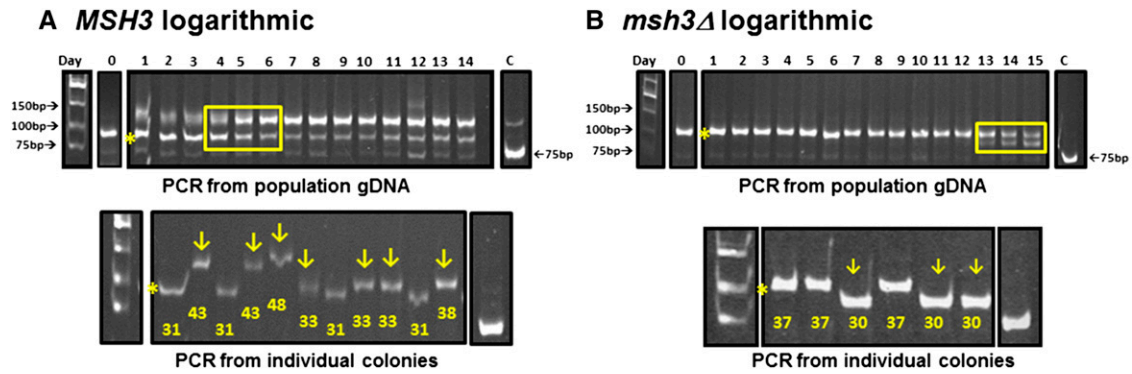

Genotype	% Expanded (Day 7)	% Expanded (Day 14)
MSH3 $(CTG)_{30}$	40% (8/20)	45% (9/20)
MSH3 $(CTG)_{34}$	45% (9/20)	45% (9/20)
MSH3 $(CTG)_{33}$	45% (9/20)	50% (10/20)
Total	**43% (26/60)**	**47% (28/60)**
MSH3 $(CAG)_{47}$	37% (11/30)	70% (14/20)
MSH3 $(CAG)_{59}$	47% (14/30)	85% (17/20)
Total	**42% (25/60)**	**78% (31/40)**

Genotype	% Expanded (Day 7)	% Expanded (Day 14)
msh3Δ $(CTG)_{32}$	15% (3/20)	15% (3/20)
msh3Δ $(CTG)_{34}$	10% (2/20)	15% (3/20)
msh3Δ $(CTG)_{33}$	0% (0/20)	5% (1/20)
Total	**8% (5/60)**	**12% (7/60)**
msh3Δ $(CAG)_{41}$	0% (0/20)	0% (0/20)
msh3Δ $(CAG)_{48}$	5% (1/20)	10% (2/20)
msh3Δ $(CAG)_{30}$	0% (0/20)	5% (1/20)
Total	**1% (1/60)**	**5% (3/60)**

Figure 4 Liquid time course experiments in *MSH3* and *msh3Δ* logarithmic cultures to determine population tract dynamics. TNR expansion events in the *MSH3* or *msh3Δ* background were selected and confirmed by PCR (see *Materials and Methods*) and log-phase cultures were established from individual isolates (see Figure 3 for cartoon). (A) *MSH3(CTG)*. (B) *msh3Δ(CTG)*. Top: The TNR tract from gDNA isolated from the *MSH3* log-phase cultures was amplified, digested, and analyzed by electrophoresis. In these examples, the initial expansion (indicated by the asterisk) contained 31 repeats for *MSH3* and 37 repeats for *msh3Δ*. The numbers across the top of the gel indicate the day of the time course. The boxed region in A (*MSH3*) indicates the progressive accumulation of a larger tract. The boxed region in B (*msh3Δ)* indicates contraction events that result in a smaller tract. The cultures went through approximately six generations in a 24-hr period (see *Materials and Methods*). Middle: Samples from day 14 cultures were plated on minimal medium lacking histidine to obtain individual colonies. Colony PCR was performed to amplify the TNR tract from colonies to determine individual tract lengths within the population. The arrows indicate tracts that have incurred an additional expansion. The number below each tract indicates the number of repeats within each tract. Control PCR reactions using the TNR plasmid (C) were performed alongside each set as a marker for the 75-base-pair tract (25 repeats). We occasionally observed higher-molecular-weight products with the control plasmid, but these represent a minor population of ≤15% of the total PCR product (Figure S2 and Figure S3). The asterisk indicates the predominant expansion product in the starting culture. Bottom: Summary of expansion frequency on days 7 and 14 in the different genetic backgrounds tested based on PCR amplification of tracts from individual colonies.

of generations (Figure 10 and Figure 11). In each case, approximate rates of tract changes were determined (Table 1). Combined, these three approaches allowed us to monitor tract length dynamics through multiple generations to document the types of tract changes that occurred *in vivo* and the rates at which they occurred. Each set of experiments was done in the presence and absence of *MSH3* to determine its role in tract dynamic behavior.

Prior to selecting for expansion events, colonies were screened for unexpanded tracts by colony PCR (Miret *et al.* 1998; Dixon *et al.* 2004; Kantartzis *et al.* 2012). In the process of screening the tracts, we noted differences between the *MSH3* and *msh3Δ* strain backgrounds. The ratio of unexpanded, expanded, and contracted tracts was significantly different in the *MSH3 vs.* the *msh3Δ* strains (χ^2: $P = 0.0038$). In particular, the relative ratios of expanded to unexpanded tracts and expanded to contracted tracts were significantly higher in *MSH3 vs. msh3Δ* strains (Fisher's exact test: $P = 0.0073$ and 0.0061, respectively), consistent with a role for *MSH3* in promoting TNR expansions. These data also indicated that *msh3Δ* strains exhibit an increase in contraction events, as suggested previously (Schweitzer and Livingston 1997; Castel *et al.* 2010).

Distinct expansion tracts in CAG and CTG repeat tracts

To measure the size of each *initial expansion event* in *CTG* and *CAG* tracts, the TNR tract from a 5-FOA-resistant colony was amplified by PCR (Miret *et al.* 1998; Dixon *et al.* 2004; Kantartzis *et al.* 2012), and the product was digested with *Sph*I and *Afl*II (see *Materials and Methods*), generating a DNA fragment that contains only the TNR tract. Although PCR has been used extensively to examine TNR tract sizes (Zhang *et al.* 1994; Leeflang *et al.* 1995, 1999; Miret *et al.* 1998; Dixon *et al.* 2004), we performed several controls to demonstrate that the observed expansions were not PCR artifacts (see *Materials and Methods*) (Figure S2, Figure S3, Figure S4, and Figure S5). With an unexpanded tract, the PCR product is 75 base pairs (25 *CNG* repeats); an expanded tract is larger, and a contracted tract is smaller (Figure S3). The size of each fragment was interpolated from

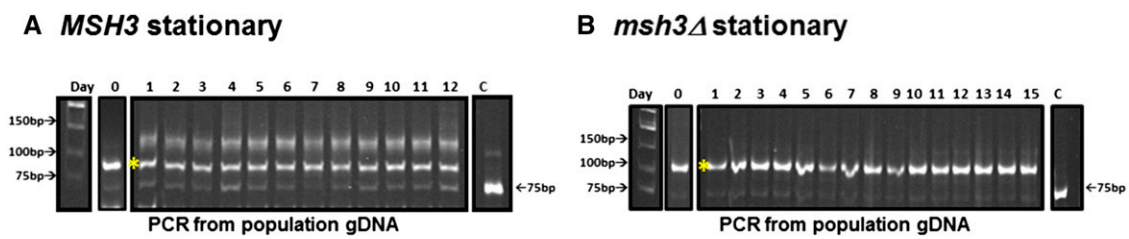

Genotype	% Expanded (Day 7)	% Expanded (Day 14)
MSH3 $(CTG)_{30}$	0% (0/20)	0% (0/20)
MSH3 $(CTG)_{34}$	10% (2/20)	10% (2/20)
MSH3 $(CTG)_{33}$	10% (2/20)	15% (3/20)
Total	**7% (4/60)**	**8% (5/60)**
MSH3 $(CAG)_{47}$	5% (1/20)	5% (1/20)
MSH3 $(CAG)_{59}$	15% (3/20)	25% (5/20)
MSH3 $(CAG)_{48}$	15% (3/20)	15% (3/20)
Total	**12% (7/60)**	**15% (9/60)**

Genotype	% Expanded (Day 7)	% Expanded (Day 14)
msh3Δ $(CTG)_{32}$	10% (2/20)	0% (0/20)
msh3Δ $(CTG)_{34}$	5% (1/20)	5% (1/20)
msh3Δ $(CTG)_{33}$	10% (2/20)	0% (0/20)
Total	**8% (5/60)**	**1% (1/60)**
msh3Δ $(CAG)_{41}$	0% (0/20)	0%(0/20)
msh3Δ $(CAG)_{48}$	0% (0/20)	0%(0/20)
msh3Δ $(CAG)_{30}$	0% (0/20)	0%(0/20)
Total	**0% (0/60)**	**0%(0/60)**

Figure 5 Liquid time course experiments in *MSH3* and *msh3Δ* stationary-phase cultures to determine population tract dynamics. Stationary-phase cultures were maintained in parallel with log-phase cultures (see Figure 3 for cartoon). The examples shown here for (A) *MSH3* and (B) *msh3Δ* match those shown in Figure 3. Top: The TNR tract was amplified from gDNA isolated from the stationary-phase culture, digested, and analyzed by electrophoresis. In both *MSH3* and *msh3Δ*, the population remained unchanged over time. The numbers across the top of the gel indicate the day of the time course. Middle: Samples from day 14 cultures were plated on minimal medium lacking histidine to obtain individual colonies. Colony PCR was performed to amplify individual TNR tracts from the stationary-phase population to determine tract lengths. These tracts were quite stable. Control PCR reactions using the TNR plasmid (C) were performed alongside each set. The asterisk indicates the predominant expansion product in the starting culture. Bottom: Summary of expansion frequency on days 7 and 14 in the different genetic backgrounds tested based on PCR amplification of tracts from individual colonies. For more detail, see Table S4.

a standard curve generated by the migration of low-molecular-weight DNA standards (New England Biolabs) electrophoresed alongside the PCR products.

In *MSH3* cells, the median size of the initial expansion event, *i.e.*, the expansion observed following selection on 5-FOA medium, was 42 repeats for the *CAG* tract (range 31–67 repeats) and 33 repeats for the *CTG* tract (range 26–43 repeats) (Figure 2 and Table S2), an increase of 17 and 8 repeats, respectively. The larger expansion size in the presence of the *CAG* tract is consistent with previous work (Miret *et al.* 1998) and is likely due to the relative stability of *CTG* and *CAG* secondary structures. *CAG* repeats form less stable structures than *CTG* repeats (Marquis Gacy *et al.* 1995; Pearson and Sinden 1996; Bacolla *et al.* 2008), and therefore, a larger expansion is predicted to be required to stabilize the secondary structure sufficiently to promote an expansion (Miret *et al.* 1998). Importantly, these size ranges put the tracts near the pathogenic threshold for *CAG* and *CTG* repeats in coding regions in humans (Figure 1) (Leeflang *et al.* 1999; Castel *et al.* 2010; McMurray 2010).

In two different *msh3Δ* backgrounds (see *Materials and Methods*) (Table S1), expansion events were less frequent, as reported previously (Kantartzis *et al.* 2012). The median initial tract length was 31 repeats in the *CAG* tract (range 31–48 repeats) and 33.5 in the *CTG* tract (range 28–39 repeats), an increase of 6 and 8 repeats, respectively (Figure 2 and Table S2). It is unclear why the size of the *CAG* tract initial expansion is significantly smaller in the *msh3Δ vs.* the *MSH3* background (Figure 2), while the *CTG* tract expansions were comparable in both backgrounds.

Expanded TNR tracts continue to expand in vivo

Using the same yeast reporter system, Rolfsmeier *et al.* (2001) demonstrated increased rates of *CTG* tract expansions and contractions as tract length increased. Therefore, we predicted that the initial expansion events that we observed, all ≥29 repeats, similarly would be less stable than the 25-repeat tract, increasing the probability of observing additional expansion events over time. However, although we can select for the initial expansion event, it is not possible to select for *additional* expansion events in this system. Therefore, to test the feasibility of screening expanded *CAG* and *CTG* tracts for additional expansions, we performed 14-day time course experiments in parallel liquid cultures (Figure 3). Three

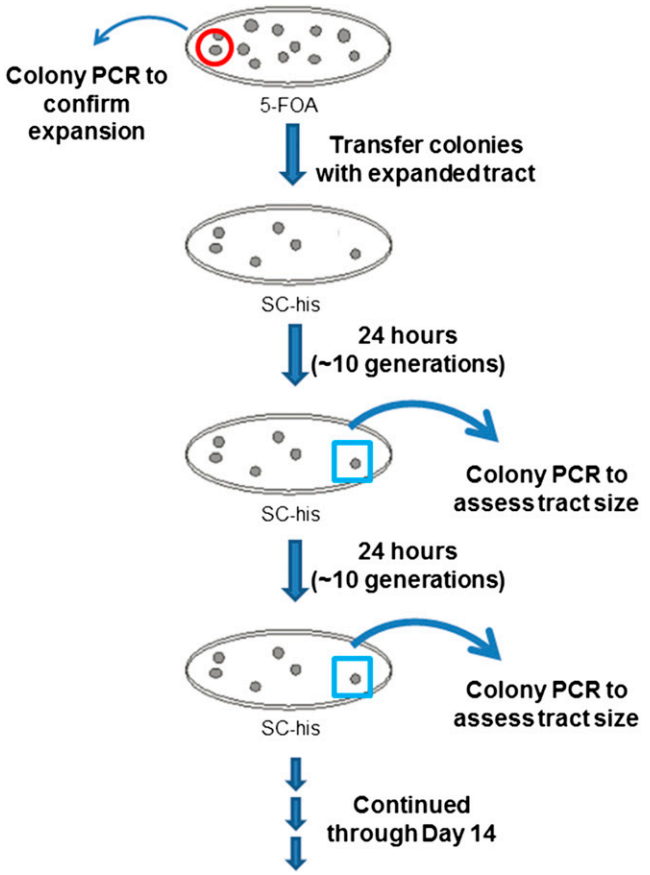

Figure 6 Schematic of the colony time course experiment protocol. Individual colonies with TNR tract expansions were selected on plates containing 5-FOA; the tract increase was confirmed by colony PCR in each case. A single colony with an expanded tract was transferred to nonselective medium and allowed to continue to grow. For each time course, the same colony was subjected to colony PCR every 24 hr (~10 generations), sampling from the perimeter of the colony where the cells continued to grow. This approach allowed us to examine the dynamics of a single TNR tract as a function of time. Because the PCR is derived from a subsample of an actively dividing colony, we are necessarily examining a mixed population, albeit derived from the same original cell. See *Materials and Methods* for additional details.

independent isolates (single colonies) with expanded *CAG* or *CTG* repeat tracts in *MSH3* or *msh3Δ* backgrounds, representing a single initial expansion event (day 0 in Figure 4 and Figure 5), were selected and used to inoculate starting cultures for a total of 12 independent time course experiments. Isolates with different initial tract sizes were selected for these experiments (Table S2). The growth curves of *MSH3* and *msh3Δ* strains carrying either *CAG* or *CTG* repeat tracts were indistinguishable (Figure S1 and data not shown); the cells went through approximately six generations every 24 hr. From each starter culture, we established parallel log- and stationary-phase cultures in liquid medium (Figure 3).

gDNA was isolated from each log- and stationary-phase culture every 24 hr and used as a template for PCR to assess TNR tract sizes within the population of the culture. A representative time course is shown in Figure 4A (top). Cells from each culture also were plated at days 7 and 14; individual colonies were used as a template for colony PCR to amplify individual TNR tracts at different time points (Figure 4B, middle). There was no selection for expansion events during the time course, *i.e.*, no 5-FOA. Therefore, the tracts were free to remain stable, to expand, or to contract.

In the *MSH3* background, the cells readily accumulated additional expansions in actively dividing cells (Figure 4); tracts in stationary cultures were substantially more stable (see next subsection). In both *CAG* and *CTG* tract time courses, analysis of the gDNA revealed that the tract size exhibited a general shift in the population to a larger size (Figure 4A, top). The band representing the major initial expansion event of 31 repeats (asterisk in Figure 4A) became less prominent over the time course. At the same time, a higher-molecular-weight product accumulated and became more prominent as the time course progressed. We note that the larger fragment was present at the beginning of the time course, presumably due to additional expansion events that occurred during the 3 days required to bring the cultures to saturation prior to setting up parallel cultures (see *Materials and Methods*) (Figure 3). Two lines of evidence suggest that this pattern is not a result of a selective advantage of cells with larger repeat tracts. First, there were only about six generations from one time point to the next (Figure S1). Second, we performed plasmid retention assays in which cells with short tracts were transformed with a plasmid conferring resistance to ClonNAT and cells containing a long tract were transformed with a plasmid conferring resistance to G418. Equal numbers of each cell type were mixed and allowed to grow in the absence of selection for 6 days. Both plasmids were present at a 1:1 ratio throughout the time course (Figure S6), indicating that neither strain has a selective advantage.

To determine whether the higher-molecular-weight tract represented (1) a single-larger expansion event that accumulates within the population over time or (2) an average of multiple different-sized expansion events within the population, we performed colony PCR on individual colonies plated on days 7 and 14. Colony PCR clearly demonstrated that a variety of tract lengths existed within the population (Figure 4A, middle) indicating multiple independent expansion events. *CTG* tracts from individual colonies revealed that 43 and 47% of the *CTG* tracts had sustained an additional expansion event at days 7 and 14 of the time course, respectively. Similarly, the *CAG* tracts exhibited a high frequency of additional expansion: 42 and 78% expansion at days 7 and 14, respectively (Figure 4A, bottom). These frequencies and the growth rate, allowed us to calculate expansion rates of 1.2×10^{-3} per cell generation (95% C.I.: 9.0×10^{-4} to 1.6×10^{-3}) for *MSH3(CTG)* and 3.1×10^{-3} (95% C.I.: 2.4×10^{-3} to 3.4×10^{-3}) per cell generation in the *MSH3(CAG)* background (Table 1). These rates are approximately two orders of magnitude higher than we observed when we performed time courses starting with unexpanded $(CTG)_{25}$ or $(CAG)_{25}$ tracts (Table 1 and Figure S7). Notably, the rates of *initial* expansion (*i.e.*, starting with an unexpanded

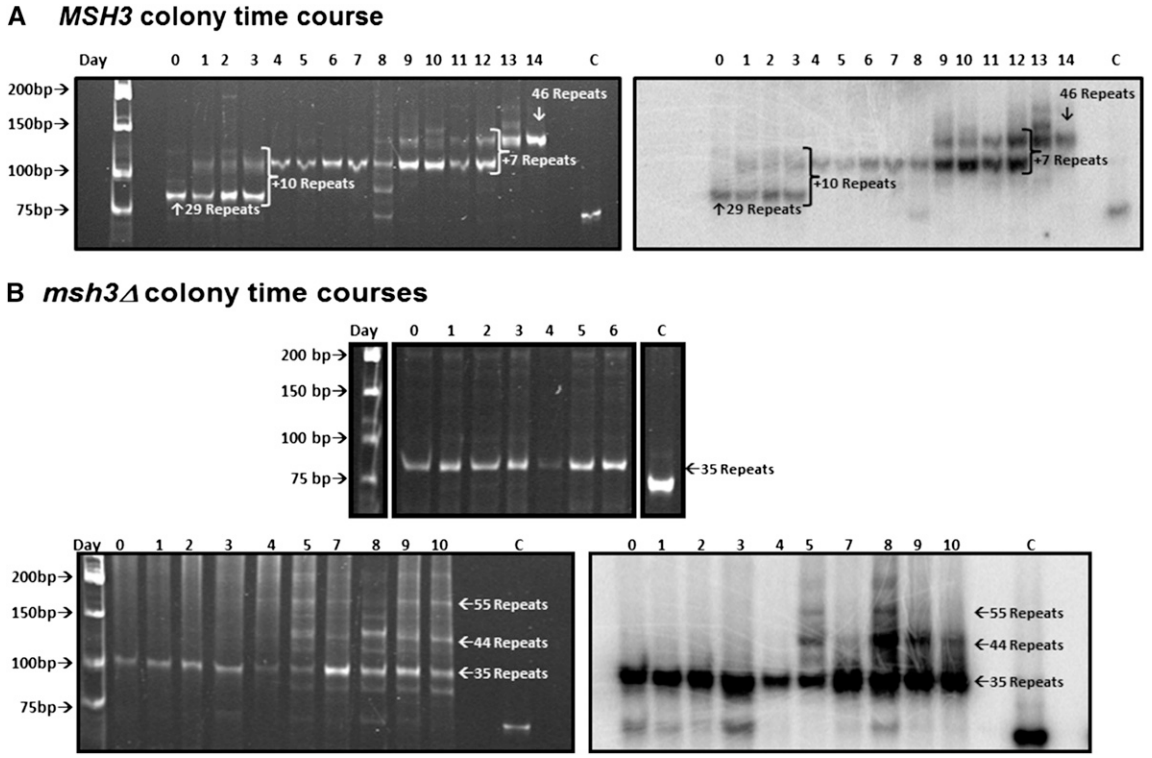

Figure 7 Progressive expansion events in *MSH3* but not in *msh3Δ*. A. *MSH3*. Expansion events were selected in the $MSH3(CTG)_{25}$ background and confirmed by PCR. Individual colonies were followed over several days; colony PCR was performed on each colony every 24 hr for 14 days to amplify the TNR tract (see Figure 6 for cartoon). Left: The tracts from time course E4 were resolved on a 12% polyacrylamide gel and stained with EtBr. The numbers across the top of the gel indicate the day of the time course. Right: Southern blot of the gel in left panel to demonstrate that the expansion products contain TNR sequence. The lanes marked C in each panel indicate the 75-base-pair tract amplified from the TNR plasmid control. (B) *msh3Δ*. Expansion events were selected in the $msh3\Delta(CTG)_{25}$ background and confirmed by PCR. Individual colonies were followed over several days; colony PCR was performed on each colony every 24 hr for 10 days to amplify the TNR tract. Top: The tracts from time course V1 were resolved on a 12% polyacrylamide gel and strained with EtBr. The numbers across the top of the gel indicate the day of the time course. Bottom left: The tracts from time course C8 were resolved on a 12% polyacrylamide gel and stained with EtBr. The numbers across the top of the gel indicate the day of the time course. Bottom right: Southern blot of the gel in lower left panel to demonstrate that the expansion products indicated by the arrows contain TNR sequence. The lanes marked C in each panel indicate the 75-base-pair tract amplified from the TNR plasmid control.

tract) in the time course assays performed here were consistent with our previous measurements for the initial expansions using the selective assay (Kantartzis *et al.* 2012). These data indicate that small increases in tract length significantly increase the rate of expansion. Furthermore, these rates may be underestimates; the further expanded tracts that we observed could have arisen through more than one expansion event. It is noteworthy that the *CAG* tract, which has a lower expansion rate when starting at 25 repeats (Miret *et al.* 1998; Kantartzis *et al.* 2012), was more likely to continue expanding than the *CTG* tract, perhaps a result of the longer starting tract sizes, consistent with the idea that stability of the secondary structure that forms within the tract affects the probability of expansion (Miret *et al.* 1998; Rolfsmeier *et al.* 2001). Once the *CAG* tract has increased sufficiently to generate a more stable secondary structure, it expands at least as rapidly as the *CTG* repeat tract.

Expanded tracts are more stable in msh3Δ background

In contrast to the *MSH3* strains, both *CAG* and *CTG* expanded tracts in the *msh3Δ* strains were much more stable when propagated in liquid culture (Figure 4B). We observed no additional expansions in the *msh3Δ* background when the gDNA was analyzed (Figure 4B, top, and data not shown). Intriguingly, analysis of the gDNA from one *msh3Δ* time course revealed contraction events starting on day 12 (Figure 4B, top). Colony PCR of tracts derived from individual cells similarly revealed very few additional expansion events (12% for *CTG* tracts, 5% for *CAG* tracts) (Figure 4B, middle and bottom); the *CTG* tracts were as likely to contract as to expand (12% expansions *vs.* 8% contractions). The expansion rate for $msh3\Delta(CTG)$ was 3.1×10^{-4} per cell generation (95% C.I.: 1.3×10^{-4} to 6.0×10^{-4}), fourfold lower that in the *MSH3* background. Similarly, the expansion rate in the $msh3\Delta(CAG)$ background was ~20-fold lower than in *MSH3* strains at 1.3×10^{-4} (95% C.I.: 2.9×10^{-5} to 3.7×10^{-4}) per cell generation (Table 1).

These data demonstrate that CNG repeat tracts become increasingly unstable and much more susceptible to expansion once they have crossed the "stability" threshold, *i.e.*, ≥29 repeats in this system, particularly in the presence of *MSH3*. These data also indicate that the presence of *MSH3*

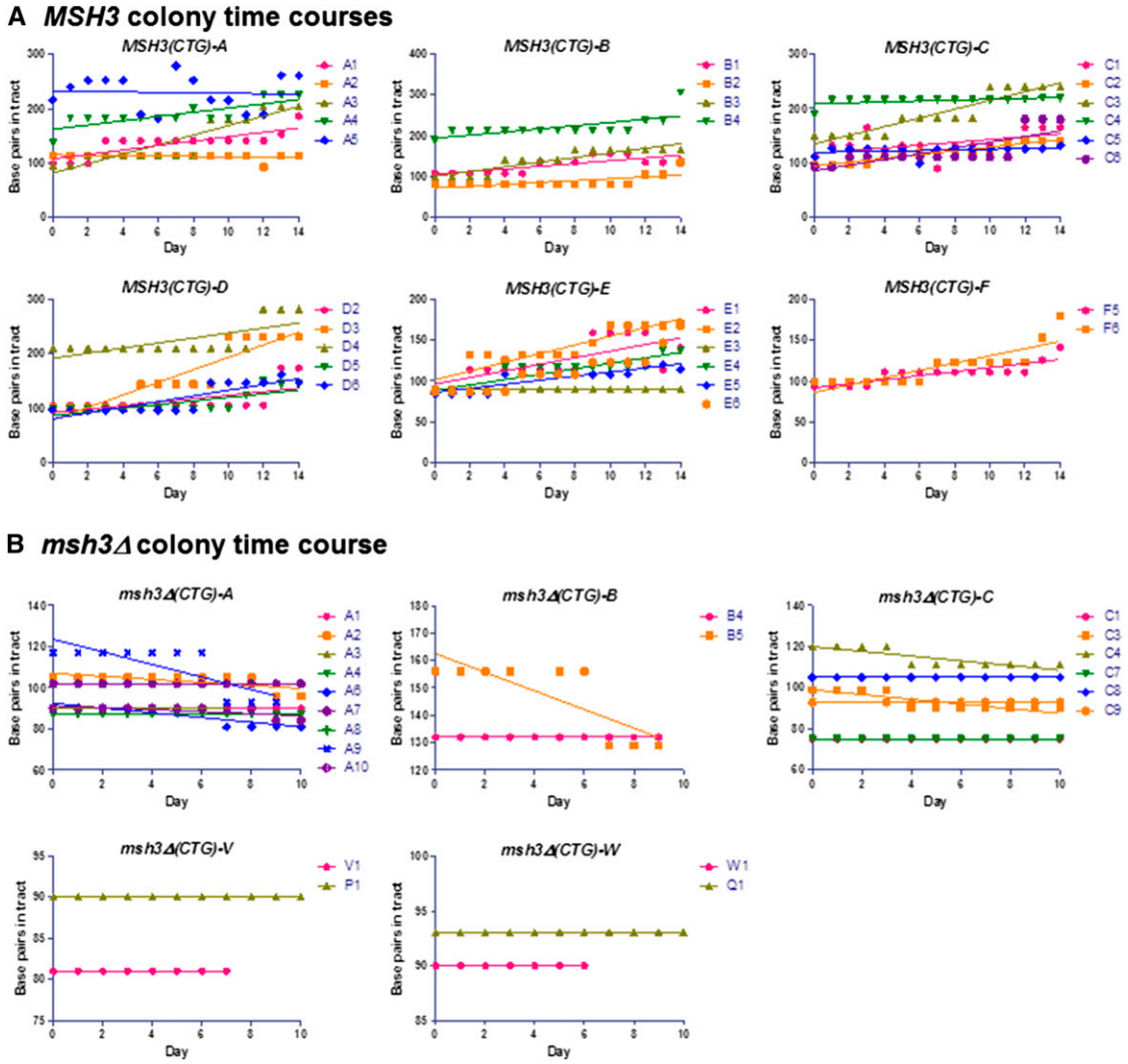

Figure 8 Colony time courses in *MSH3* and *msh3Δ* backgrounds. The TNR tract size was plotted as a function of time to demonstrate trends in the data. Each panel represents an independent $(CTG)_{25}$ integrant in the different strain backgrounds. Each curve in a single panel represents the time course of an independent expansion event in that background. (A) *MSH3*. All *MSH3* colony time courses were plotted. Each plot shows the tract size changes in independent colonies from a single $MSH3(CTG)_{25}$ isolate. A total of 64 time courses were performed: 28 showed progressive expansion, 3 showed tract stability, 11 showed no amplification (loss of tract), and 22 showed high background with multiple PCR products. This last category was difficult to interpret but exhibited trends similar to those analyzed in Figure 8A; 9 tracts exhibited increasing trends, and 4 tracts appeared stable. (B) *msh3Δ*. All *msh3Δ* time courses were plotted, and linear regressions were calculated. A total of 64 time courses were performed: 0 showed progressive expansion, 23 showed tract stability, 7 tracts showed contractions, 26 showed no amplification (loss of tract), and 6 showed high background with multiple PCR products. Linear regressions were plotted for each time course to illustrate the general trends in tract length.

promotes not only the initial expansion event (or events) that allow for selection in this system but also subsequent expansion events, at least within this threshold range. Therefore, we can use expanded tracts as a starting point to examine tract dynamics; there are likely to be changes within a time frame of several days. Furthermore, the initial expansions are relatively small, increasing to a total of ≤50 repeats and representing early events in the progression of an expanded tract.

Expansions were enhanced in dividing cells

In contrast to *CNG* repeat tracts in replicating cells, the tracts from the stationary-phase cultures in both the *MSH3* and *msh3Δ* backgrounds were more stable (Figure 5), indicating that a significant proportion of the expansion events depend on DNA replication. Based on analysis of the gDNA from *MSH3* cultures, the major initial expansion event (asterisk) remains the major PCR product throughout the time course; there is little or no accumulation of additional expansion events (Figure 5A, top). Colony PCR from individual colonies similarly revealed that the tracts were very stable in stationary phase (Figure 5A, middle and bottom). We observed that 7 and 8% of the *CTG* tracts were further expanded on days 7 and 14, respectively, while 12 and 15% of the *CAG* tracts had additional expansions on days 7 and 14, respectively.

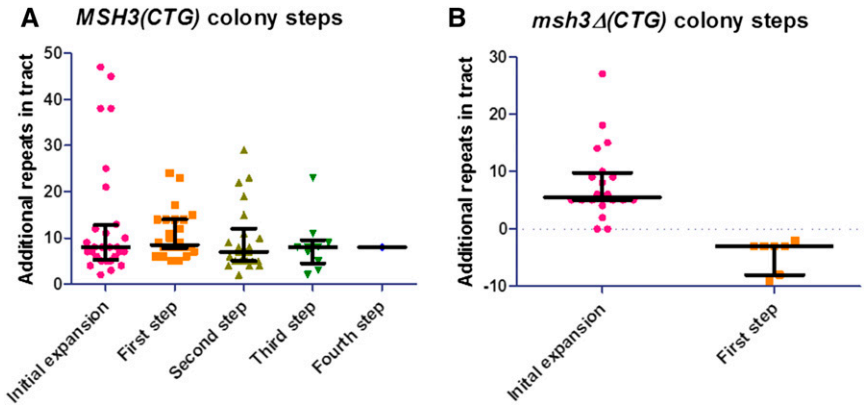

Figure 9 Sizes of each step (tract size change) in colony time course experiments. Each progressive tract length change, defined as the loss of one tract length and the concomitant appearance of a different tract length, was plotted as a function of size for *MSH3* (A) and *msh3Δ* (B) using GraphPad Prism. The median and interquartile ranges for each step are indicated in black. (A) *MSH3*. The initial expansion size selected on 5-FOA is indicated (pink circles). The orange squares indicate the size of each individual tract upon the first tract length change or step. Similarly, the second, third, and fourth steps are shown (olive triangles, green inverted triangles, and blue diamonds, respectively). The median size of each step is essentially unchanged. (B) *msh3Δ*. The sizes of the initial expansion events are shown (pick circles); the median is comparable to that of the *MSH3* time courses. Only one progressive step was observed (orange squares), and this was a step down to a short tract length.

The frequency of expansions in the *msh3Δ* background also was lower in the stationary-phase cultures (Figure 5B). There were neither expansions nor contractions when the gDNA was analyzed. And there were very few additional expansions observed from the colony PCR analysis, again confirming that DNA replication is important in promoting these additional expansion events. We do note, however, that even in the stationary phase, there were more additional expansion events in the *MSH3* background than in the *msh3Δ* background. With the *CTG* tract, we observed 8 and 1% expansions on days 7 and 14, respectively; we observed no expansions in the *CAG* stationary phase cultures (Figure 5B, bottom). This is consistent with the observation that Msh2-Msh3 promotes *CNG* expansions in postmitotic (nondividing) tissues in mammalian systems (McMurray 2010; Kovalenko *et al.* 2012).

Expanded TNR tracts increase in discrete steps

To follow tract dynamics as a function of time, we selected independent expanded tracts on 5-FOA medium and confirmed their sizes by PCR, as described earlier. Colonies with a range of initial tract sizes (*i.e.*, initial expansion events) were selected for further analysis . We chose to focus on *CTG* tracts because the range of initial expansion events was more similar in the *MSH3* and *msh3Δ* backgrounds than with *CAG* tracts (Figure 2 and Table S2). Each colony was then transferred to nonselective medium (no 5-FOA) so that the tract was free to expand or contract (Figure 6). Colony PCR was performed on the same colony every 24 hr for 10–14 days to assess tract length. Additional expansions were observed in most of the time courses, and the increase in the size of the tract was progressive (Figures 7A and Figure 8A). While multiple tract sizes often were observed at the same time point, the overall size of the predominant tract increased over time, with a concomitant loss of the smaller-sized tracts. We refer to this as a *progressive tract length change*. Typically, two–three discrete progressive changes, or increments, were observed over 14 days, indicating that the expansions occur in steps. We confirmed that these PCR

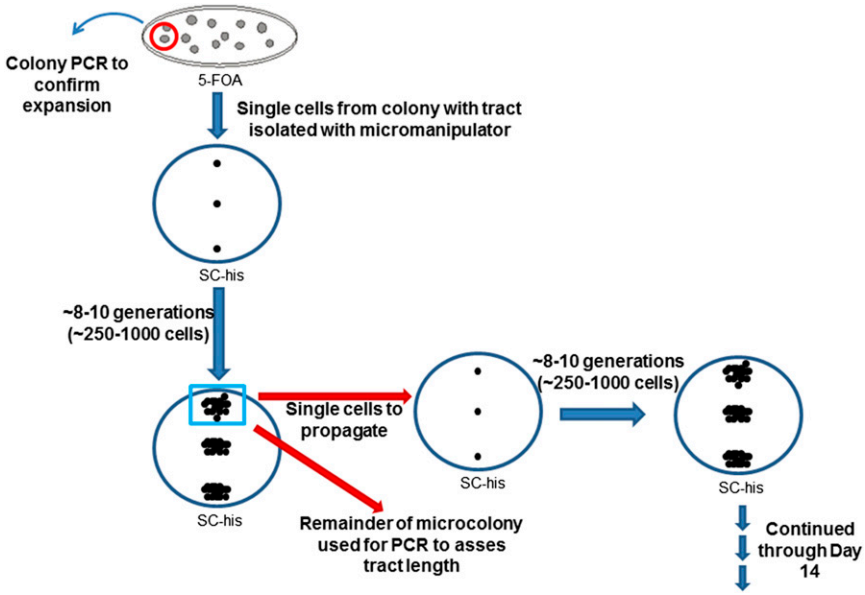

Figure 10 Schematic of the microcolony time course experiment protocol. Individual colonies with TNR tract expansions were selected on plates containing 5-FOA; the tract increase was confirmed by colony PCR in each case. Instead of initiating the time course with a potentially mixed population, the microcolony time course was started with single cells from a colony with an expanded tract. These cells were restricted to between 8 and 10 cell divisions, with an eye to minimizing the heterogeneity within the population. See *Materials and Methods* for additional details.

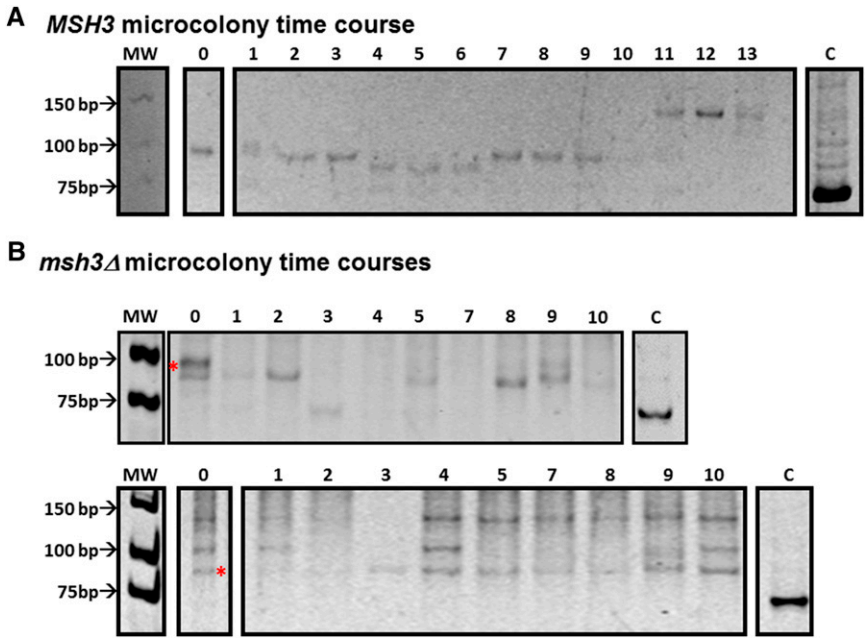

Figure 11 Dynamic changes in TNR tracts starting from a single cell. Expansion events were selected in either the *MSH3*$(CTG)_{25}$ (A) or *msh3Δ*$(CTG)_{25}$ (B) background and confirmed by PCR. Individual cells from these colonies were isolated and allowed to undergo 8–10 rounds of replication, resulting in a microcolony approximately 250–1000 cells in size. A single cell was then taken from this microcolony to propagate another microcolony. The remainder was used to amplify the TNR tract by PCR to determine tract length (see Figure 10 for cartoon). (A) An example of TNR tract dynamics in an *MSH3* microcolony (F from Table 2). There are multiple changes in the TNR tract over time. (B) Two examples of TNR tract dynamics in an *msh3Δ* microcolony (N and Q, respectively, from Table 3). The red asterisk indicates the position of the initial expansion tract size, as determined by Southern blot. The upper bands in the bottom panel do not contain TNR tract sequences, as determined by Southern blot (data not shown). The tract appears more stable than in the *MSH3* background. Both gels are 12% polyacrylamide gels stained with EtBr; the images of been inverted for ease of viewing. The lanes marked C in each panel indicate the 75-base-pair tract amplified from the TNR plasmid control. The numbers across the top of the gels indicate the time point.

products contained the TNR tract by Southern blot using a tract-specific (*CTG*) probe (Figure 7A, right). We also performed PCR controls to rule out the possibility that larger tracts were preferentially amplified (see *Materials and Methods*) (Figure S5).

In Figure 8A, we plotted the progressive changes in tract length as a function of time for all the *MSH3(CTG)* time courses that we evaluated. There is a clear upward trend in tract length in most of the time courses, although contractions and stable tracts are also evident. Importantly, these changes were discrete increases in size, which we refer to as *steps*. Overall, the tracts appeared to expand in relatively small increments, or steps, over time (Figure 7A and Figure 8A). Even cells with very large initial expansions exhibited incremental increases in this range. For example, two colonies (Figure 8A, B4 and C4) with initial expansions of 38 repeats (for total lengths of 63 repeats) had subsequent increases of only 8 and 9 repeat lengths, respectively. Conversely, one 70-repeat tract (Figure 8A, D4) sustained a 24-repeat increase. Therefore, in our data set, there does not seem to be a strict correlation between tract length and the size of additional expansion events in the tract length range that we investigated. All the increases were smaller than the initial tract length. These data therefore suggest that the longer tract expansions are the result of multiple expansion events.

To assess the size of each step and determine whether there is a correlation in step size with respect to starting tract length, we plotted the number of additional repeat units we observed at each tract length change for all the time courses plotted in Figure 8A (Figure 9A). Thus, the pink circles demonstrate the number of repeat units we observed in each initial expansion event, *i.e.*, after selection on 5-FOA. The median size of the initial expansion was 24 base pairs (8 repeats). An additional increase in tract length, *i.e.*, the first step beyond the initial expansion, was plotted using the orange squares, and the subsequent increases, or second, third, and fourth steps, were similarly plotted. Thus, only the time courses that exhibited progressive tract length changes are represented in this figure. We note that there was not a strict correlation in the timing of the tract length changes (Figure 8A), and therefore, the size of the tract changes was plotted independent of time point. When all expansions were taken into account, the median size of the tract length increase, or step, was 24 base pairs (8 repeats); the average increase was 11 repeats ($\pm$18 repeats, 2 SD), but the range was large: 2–47 repeats. The median size of each step was 8 repeats and did not increase with increasing tract size within the range of tract lengths that we observed (Figure 9A). In fact, the increase in tract size decreased after the initial expansion, as did the range in expansion events.

When individual *msh3Δ* colonies with an expanded TNR tract were followed over time, the TNR tracts appeared more stable (Figures 7B, Figure 8B, and Figure 9B), consistent with our observations in the population-based time course (Figure 4). In 64 time courses, we observed no evidence of progressive expansion (Figures 7B and Figure 8B), as defined earlier with the concomitant loss of the smaller tract length. We did observe additional PCR products in some cases, but this resulted in a mixed population, with $\geq$75% of the tract remaining at the original expansion size (Figure 7B). The results of the mixing experiments (Figure

Table 1 Summary of rates of tract length change calculated from liquid, colony, and microcolony time courses

Genotype	Rates of tract length changes		
	Liquid[a] (95% C.I.)[b]	Colony (95% C.I.)	Microcolony (95% C.I)
MSH3(CTG)	1.2×10^{-3} (9.0×10^{-4} to 1.6×10^{-3})	1.5×10^{-2} (1.2×10^{-2} to 1.9×10^{-2})	3.5×10^{-2} (2.8×10^{-2} to 4.2×10^{-2})[e]
MSH3(CAG)	3.1×10^{-3} (2.4×10^{-3} to 3.4×10^{-3})	ND[c]	ND
msh3Δ(CTG)	3.1×10^{-4} (1.3×10^{-4} to 6.0×10^{-4})	3.6×10^{-3} (1.5×10^{-3} to 7.2×10^{-3})[d]	1.6×10^{-2} (1.1×10^{-2} to 2.2×10^{-2})[f]
msh3Δ(CAG)	1.3×10^{-4} (2.9×10^{-4} to 3.7×10^{-4})	ND	ND
$MSH3(CTG)_{25}$	$<5 \times 10^{-5}$[g,h]	ND	$<1.2 \times 10^{-3}$[g,h]
$MSH3(CAG)_{25}$	5.1×10^{-5}[h]	ND	ND

[a] Expansions only.
[b] 95% C.I.s determined by *F*-statistic.
[c] Not determined.
[d] Predominantly contractions.
[e] Slight bias toward expansions.
[f] Bias toward contractions.
[g] No tract changes observed.
[h] Low numbers precluded accurate calculation of 95% C.I.

S5B) suggest that this ratio indicates an approximately five-fold excess of unexpanded tract template in the reaction. In these events, we observed a total of one–two tract species in addition to the original tract size, which continued to dominate the population. We also observed contractions of the predominant PCR product in seven independent time courses (Figure 8B). In contrast, no *progressive* contractions were observed in the *MSH3* background, although some individual contractions were observed (Figure 8A). Southern blotting confirmed the presence of the *CTG* tract in each of these DNA fragments (Figure 7B and data not shown). Overall, taking only progressive tract length changes into account, the rate of change in tract length in *msh3Δ* cells was 3.6×10^{-3} per generation (95% C.I.: 1.5×10^{-3} to 7.2×10^{-3}); the changes observed were all contractions. In contrast, the rate of tract length change in *MSH3* cells, again including only progressive tract length changes, was 1.5×10^{-2} per generation (95% C.I.: 1.2×10^{-2} to 1.9×10^{-2}), fourfold higher than in the *msh3Δ* cells, and the observed changes were almost exclusively expansions (Table 1). We note that these are likely underestimates because minor expansion and contraction products were observed in both *MSH3* and *msh3Δ* time courses. Furthermore, the extent of expanded products observed may depend on the section of the colony sampled. Nonetheless, the presence of Msh2-Msh3 appears to shift the dynamic equilibrium toward expansion over time, ultimately resulting in longer and longer TNR tracts. The absence of the complex stabilizes the tract and permits an increase in contraction events, possibly as a result of the MMR deficiency (see *Discussion*).

TNR tracts are highly dynamic as they expand

The incremental expansions of the TNR tract observed within individual colonies were smaller than the tract length but were typically larger than the increments we observed *in vitro* (Kantartzis *et al.* 2012), although they were on the same order of expansions previously observed by single-sperm typing in humans (Leeflang *et al.* 1995, 1999). To determine whether each expansion event represented a single larger event or the sum of multiple small events, indicating a highly dynamic TNR tract, we initiated time courses with a single cell rather than a potentially mixed population within a colony. First, we selected a colony that contained an expanded TNR tract. From this colony we isolated individual cells using a micromanipulator (Figure 10). These single cells were allowed to go through approximately 8–10 cell divisions (and therefore 8–10 rounds of replication), resulting in a microcolony of ~250–1000 cells. Individual cells from each microcolony were selected to propagate a new microcolony to continue the time course. The remainder of the microcolony was used as a template for PCR.

In the *MSH3* background, starting with tracts between 30 and 33 repeats, we observed very dynamic behavior of the tract, with several small changes in tract size occurring over the course of 2 weeks (Figure 11A and Table 2). Multiple products were frequently observed at each time point, indicating a mixed tract population within the microcolony. We quantified the predominant tract at each time point and observed both expansions and contractions in similar quantities (slight bias toward expansions) and of similar sizes, many of which were one, two, or three TNRs in length (*i.e.*, three, six, or nine nucleotides) (Table 4). Although the total number of events is low, we calculated an approximate rate of tract size change per generation (expansions and contractions) of 3.5×10^{-2} per generation (95% C.I.: 2.8×10^{-2} to 4.2×10^{-2}), assuming 10 generations per time point (Table 1). The changes in tract size observed on this time scale were smaller than those observed in the colony time course and more closely resembled the size of expansions observed *in vitro* in the presence of Msh2-Msh3, Rad27 (Fen1), and Cdc9 (Lig1) (Kantartzis *et al.* 2012). Therefore, in a wild-type (*MSH3*) background, threshold-length TNR tracts demonstrated a tendency to gradually increase in size. Notably, even in tracts where there was no net change in tract length at the end of the time course, the tract length did change during the time course (*i.e.*, C, D, E, and G in Table 2).

In the absence of *MSH3*, the tracts appeared more stable overall (Figure 11B and Table 3), with an estimated

Table 2 *MSH3* microcolony tract dynamics

TNR tract dynamics of individual *MSH3* microcolonies															
Day	A	B	C	D	E	F[a]	G	H	I	J	M	R	P	S	9
Initial tract[b]	32	30	32	33	31	30	31	32	34	30	30	31	33	32	31
1	0[c]	0	0	5	0	2	0	0	0	0	0	0	0	0	0
2	3	0	0	−5	0	−2	0	0	0	0	0	0	0	0	0
3	−3	0	0	0	0	0	0	0	0	0	0	0	0	0	−7
4	2	−2	0	−2	−3	−2	−2	0	−3	5	0	−4	−3	0	7
5	1	0	1	3	3	0	2	−3	3	0	0	4	3	0	0
6	−1	0	0	0	2	0	0	3	0	0	0	0	0	0	1
7	1	0	−3	0	0	2	0	5	0	0	0	0	0	0	−4
8	0	0	−2	0	−7	0	8	−5	0	2	0	0	0	0	3
9	−1	0	4	0	0	0	0	−3	0	0	0	0	0	0	0
10	1	0	0	7	7	4	0	3	0	0	0	0	0	0	0
11	0	0	0	−7	−2	6	−8	0	0	2	0	0	0	0	0
12	11	0	0	−4	−2	0	−2	0	0	−2	0	0	0	0	0
13	—[d]	−1	0	—	4	0	9	14	3	5	0	4	−3	0	0
Final tract[e]	46	27	32	30	33	40	38	46	37	42	30	35	30	32	31
Net change[f]	14	−3	0	−3	2	10	7	14	3	12	0	4	−3	0	0

[a] Corresponds to gel in Figure 11A.
[b] Initial expansion size following selection in the presence of 5-FOA in number of repeats.
[c] Change in number of repeats in tract.
[d] No amplification of tract.
[e] Number of repeats.
[f] Net change in number of repeats within tract.

mutation rate per generation of 1.6×10^{-2} per generation (95% C.I.: 1.1×10^{-2} to 2.2×10^{-2}) (Table 1), half the rate observed in the presence of *MSH3*. We do note that additional PCR products were observed in some of these time courses. However these additional bands did not change in size over the course of the experiment, indicating stability. Furthermore, in several cases, including the lower panel of Figure 11B, Southern blots indicated that the upper bands did not contain TNR sequences (data not shown). When changes did occur, the median size of the increments was similar to that observed in the *MSH3* background. However, the tracts in the *msh3Δ* strains were more likely to contract than to expand (10 expansions, 18 contractions) (Table 4), in contrast to roughly equal proportions of expansions and contractions in the *MSH3* background, with a bias toward expansions (38 expansions, 30 contractions) (Table 4).

Discussion

We have, for the first time in any system, documented the dynamic behavior of threshold-length TNR tracts and tracked them over time in dividing cells. The rate of change in the size of threshold-length TNR tracts is remarkable, at two–three orders of magnitude higher than the stable $(CNG)_{25}$ repeats in yeast (Miret *et al.* 1998; Rolfsmeier *et al.* 2001; Kantartzis *et al.* 2012). Thus, small increases in tract length led to substantially higher expansion rates. The rapid rate of change in tract length, both expansions and contractions, was particularly striking when threshold-length tracts were examined in microcolonies derived from a single cell. In contrast, we did not observe similar changes in an unexpanded $(CTG)_{25}$ tract (Figure S8).

Previous studies have proposed a model for TNR expansions in dividing cells that involved incremental expansions (Leeflang *et al.* 1995, 1999; Martorell *et al.* 2004; Kantartzis *et al.* 2012). Here we have shown directly that incremental expansions do in fact occur *in vivo* within *CTG* repeat tracts. The size of the increments varies but can be as small as a single repeat unit. This is consistent with the behavior of *CAG* repeats at both the HD and androgen receptor loci in humans (Zhang *et al.* 1994; Leeflang *et al.* 1995). Recent work modeling human DM1 expansion data also has demonstrated that these expansions are likely to occur through small incremental steps (Higham *et al.* 2012; Morales *et al.* 2012; Higham and Monckton 2013). In induced pluripotent stem cells (iPSCs) from HD and DM1 patients, Du *et al.* (2013) observed that $(CAG)_{\sim 46}$ and $(CTG)_{\sim 57}$ tracts were stable after 12 and 16 passages, respectively. For comparison, yeast cells went through approximately 120 cell divisions during the 2-week time course experiments in this study. However, a larger *CTG* tract (~126 repeats) expanded by approximately one repeat increment in each passage; a $(CTG)_{\sim 773}$ tract expanded in larger increments (Du *et al.* 2013). These data are consistent with a stepwise increase in the early stages of TNR tract expansion.

Importantly, the absence of *MSH3* alters the dynamics of the tract in this model system. Overall, in actively replicating cells, both the *CAG* and *CTG* tracts are more stable in the *msh3Δ* background, consistent with previous observations (Owen *et al.* 2005; Kantartzis *et al.* 2012). Expansions did occur, but at a significantly lower rate than in the *MSH3* background, as described previously (Kantartzis *et al.* 2012). Furthermore, *msh3Δ* cells were much less likely to incur an additional expansion, and when additional expansions did

Table 3 *msh3Δ* microcolony tract dynamics

TNR tract dynamics of individual *msh3Δ* microcolonies																							
Day	A	B	C	D	E	F	G	H	I	J	K	L	M	N[a]	O	P	Q[b]	R	S	T	U	V	W
Initial tract[c]	30	31	30	30	31	32	32	32	32	29	30	30	32	30	30	36	29	29	30	30	29	29	30
1	0[d]	0	0	**0**	0	−3	−2	−2	0	0	0	0	−2	−1	0	—	0	0	0	0	0	−2	0
2	0	0	0	0	0	0	0	0	0	0	0	0	0	0	0	−7	0	0	0	0	0	0	0
3	—[e]	—	—	—	—	—	—	—	—	—	−5	0	−5	−5	—	0	0	0	—	—	0	—	—
4	—	—	—	—	0	0	0	−1	—	—	0	0	0	5	—	—	0	—	—	—	0	—	—
5	—	—	—	—	—	—	—	—	—	—	—	—	—	0	—	—	0	—	—	0	0	—	—
6	0	—	0	0	0	0	—	0	0	—	5	0	5	0	0	—	0	—	—	0	—	—	—
7	0	0	0	0	−1	0	0	0	0	0	0	0	0	—	0	0	0	0	0	0	—	0	0
8	−1	0	0	0	0	0	0	0	3	0	0	0	0	0	—	0	0	0	0	0	0	2	6
9	0	0	0	4	0	0	0	0	−3	0	0	0	0	1	0	—	0	0	—	0	0	0	0
10	0	0	0	−5	1	0	0	0	0	0	0	0	0	−1	0	0	0	0	0	0	0	—	−1
11	0	0	0	1	—	0	0	0	0	0	0	0	0	—	—	0	—	0	0	—	—	—	−4
Final tract[f]	29	31	30	30	31	29	30	31	32	29	30	30	30	29	30	29	29	29	30	30	29	31	28
Net change[g]	−1	0	0	0	0	−3	−2	−1	0	0	0	0	−2	−1	0	−7	0	0	0	0	0	0	−2

[a] Corresponds to gel in upper panel of Figure 11B.
[b] Corresponds to gel in lower panel of Figure 11B.
[c] Initial expansion size following selection in the presence of 5-FOA in number of repeats.
[d] Change in number of repeats in tract.
[e] No amplification of tract.
[f] Number of repeats.
[g] Net change in number of repeats within tract.

occur, they were less likely to become the predominant population (Figures 3–11), despite the fact that the cell division time for the two strains was indistinguishable. Therefore, loss of *MSH3* reduces the probability of incurring both an initiating and a secondary expansion event. However, contraction events were observed more frequently in *msh3Δ* strains (*e.g.*, Figure 8 and Table 4). This is consistent with the results of Schweitzer and Livingston (1997), who demonstrated an increase in TNR contractions in *msh2Δ* cells using a different yeast reporter system. The increased rate of contraction may be related to the loss of IDL MMR in the absence of *MSH3*; Msh2-Msh3 preferentially corrects deletion events, *i.e.*, loops on the template strand, during DNA replication (Schweitzer and Livingston 1997; Sia *et al.* 1997; Romanova and Crouse 2013). These observations support the suggestion that Msh3 is a potential therapeutic target (Castel *et al.* 2010) and underscore the need to develop a better understanding of tract dynamics in different genetic backgrounds. It will be of interest to determine whether the size of the contractions varies with *MSH3* status.

It is striking that in the absence of selection for tracts larger than 30 repeats, we nonetheless observed a strong bias toward expansions in the *MSH3* background with very few contractions. This is distinct from previous observations in yeast, where there was a strong bias toward contractions (Maurer *et al.* 1996; Miret *et al.* 1997; Rolfsmeier *et al.* 2001), although when expansions were observed, they were relatively small, ranging from 2 to ∼20 repeat lengths (Maurer *et al.* 1996; Miret *et al.* 1998), consistent with our observations. We performed a preliminary contraction assay and observed rates of contraction similar to those observed previously (Miret *et al.* 1997), indicating that there is nothing inherent in our strain background that predisposes toward expansions (data not shown) but rather that the sizes of the tracts themselves led to the shift toward expansions. As such, the threshold-length tract behavior that we observed in yeast mimics that which has been observed in human sperm cells and iPSCs and therefore is a good model for events in dividing cells. In this model we can look at large numbers of cells over many generations, making this a very flexible and informative approach to examining TNR tract dynamics. It is important to note that Msh2-Msh3-mediated expansions are just one mechanism by which TNR tracts increase in length. This yeast system is amenable to examining the contribution of additional genetic factors on tract dynamics in both deletion and mutation backgrounds (*e.g.*, Debacker *et al.* 2012; Concannon and Lahue 2014)).

Although this study focused on actively replicating cells, we note that the frequency of additional expansions also was elevated in stationary-phase cultures relative to the unexpanded tract (Figure 5A); ∼10–15% of the tracts had an additional expansion event in the *MSH3* background. Notably, this decreased in the absence of Msh3 (Figure 5B). Msh2-Msh3 has been shown to be important in promoting somatic tract expansions in postmitotic (nonreplicating) neurons, specifically in medium-spiny striatal neurons (MSNs) in a mouse model for HD (Kovalenko *et al.* 2012). Deletion of *Msh2* eliminated most of the *CAG* expansions in the HD gene (*HTT*) in the MSNs. The decrease in expansions correlated with a reduction in *HTT CAG*-dependent phenotypes in the mice. In another study, *Msh3* polymorphisms that altered Msh3 protein levels in mouse striatal tissues also altered the stability of the HD transgene *CAG* repeat tract: elevated Msh3 levels correlated with increased tract size (Tomé *et al.* 2013). Recent work has suggested that *CAG* expansions in somatic tissue also may occur in an incremental

Table 4 Trinucleotide repeat tract dynamics in microcolony time courses

Genotype	Type of event	Number of events	Median size of event (range in number of repeats)
MSH3(CTG)[a]	Expansion	38	3 (1–14)
	Contraction	30	3 (1–8)
		Final TNR tract length	33 (27–46)
msh3Δ(CTG)[b]	Expansion	10	3 (1–6)
	Contraction	18	2 (1–7)
		Final TNR tract length	30 (29–32)

[a] Ninety-six total time courses were initiated: 32 time courses were completed to at least day 12; of these,13 exhibited TNR tract dynamics, 2 exhibited a stable tract length, 15 exhibited no tract amplification, and 2 were uninterpretable due to high background.
[b] One-hundred and five total time courses were initiated: 37 time course were completed to at least day 10; of these, 14 exhibited TNR tract dynamics, 9 exhibited a stable tract length, and 14 exhibited no tract amplification.

manner (Lee *et al.* 2011). A cohort of HD *CAG* knock-in mice was sampled at 2, 5, 9, 12, and 16 months of age, and *CAG* tract length was examined in the liver and striatum. In these tissues, there was an average increase in tract size of one repeat per month, although there was a much broader distribution in the striatum than in the liver. *In vitro*, human Msh2-Msh3 (MutSβ) stimulated expansions in a replication-independent system (Stevens *et al.* 2013). Therefore, monitoring TNR tracts in stationary-phase yeast cultures may be a powerful way to model tract dynamics in nonproliferating cells and elucidate the mechanism(s) of expansions in somatic cells.

Although we have not tested the effect of *msh2Δ* on dynamic TNR tract behavior, our *in vivo* and *in vitro* data (Kantartzis *et al.* 2012) examining TNR tracts are consistent with a model in which TNR secondary structures are bound and stabilized by Msh2-Msh3. Increased tract length increases the probability that alternative DNA structures will form, perhaps during Okazaki fragment processing or base excision repair, leading to the recruitment of Msh2-Msh3. So why are the structures not repaired? *In vitro* work with human MutSβ (Msh2-Msh3) has indicated that the Msh2-Msh3/TNR complex is distinct from the Msh2-Msh3/loop complex (Owen *et al.* 2009; Lang *et al.* 2011). Similarly, Msh2-Msh3 exhibits distinct nucleotide turnover behavior when bound to MMR *vs.* double-strand DNA break repair (DSBR) substrates (Kumar *et al.* 2013, 2014). It is not yet clear how these proposed kinetic differences could translate into increased expansions, but we favor the possibility that Msh2-Msh3-mediated ATP-binding and hydrolysis activities are altered in the presence of the TNR substrate, disrupting error-free MMR. Altered Msh2-Msh3 activity could block repair altogether or recruit an error-prone repair process that ultimately retains the insertion. Recent work has demonstrated that mammalian MutLγ (Mlh1-Mlh3) is required for somatic *CAG* expansions in a HD mouse; MutLα (Mlh1-Pms2) was dispensable (Pinto *et al.* 2013). Intriguingly, Rogacheva *et al.* (2014) demonstrated that yeast Mlh1-Mlh3 enhances Msh2-Msh3 DNA-binding activity, while Msh2-Msh3 stimulates Mlh1-Mlh3 endonuclease activity. Therefore, enhanced Msh2-Msh3 binding to TNR structures could inappropriately recruit Mlh1-Mlh3 during replication or outside of S phase and stimulate its endonuclease activity, leading to gap formation and DNA repair synthesis that incorporates incremental expansions (Gomes-Pereira *et al.* 2004; Pluciennik *et al.* 2013).

Disruption of Msh2-Msh3 has been proposed as an attractive therapeutic target for TNR expansion disease such as HD or DM1 (Panigrahi *et al.* 2005, 2006; Castel *et al.* 2010). Loss of *MSH3* leads to a decrease in expansion events and promotes contractions. However, disruption of Msh2-Msh3 will have a negative impact on overall genome stability; in addition to MMR, Msh2-Msh3 has been implicated in DSBR (Surtees *et al.* 2004; Park *et al.* 2013; van Oers *et al.* 2013) and interstrand DNA cross-link repair (Takahashi *et al.* 2011; Barber *et al.* 2005; Zhao *et al.* 2009). Notably, many neuronally expressed genes contain repetitive sequences in their regulatory regions (Bacolla *et al.* 2008), the stability of which is likely at least partially dependent on Msh2-Msh3. Therefore, in considering Msh2-Msh3 as a molecular target, a clear mechanistic understanding of Msh2-Msh3 function in promoting repeats is vital to ensure that a balance is struck between promoting genome stability and genome instability in developing rational therapeutic strategies.

Acknowledgments

We are grateful to Mark Sutton, Robert Lahue, Catherine Freudenreich, and Eric Alani for comments on this manuscript and to members of the Surtees Laboratory for discussions of this work. Work in the Surtees Laboratory is supported by National Institutes of Health grant GM-087459. The funder had no role in study design, data collection and analysis, decision to publish, or preparation of the manuscript.

Literature Cited

Alani, E., L. Cao, and N. Kleckner, 1987 A method for gene disruption that allows repeated use of URA3 selection in the construction of multiply disrupted yeast strains. Genetics 116: 541–545.

Bacolla, A., J. E. Larson, J. R. Collins, J. Li, A. Milosavljevic *et al.*, 2008 Abundance and length of simple repeats in vertebrate genomes are determined by their structural properties. Genome Res. 18: 1545–1553.

Barber, L. J., T. A. Ward, J. A. Hartley, and P. J. McHugh, 2005 DNA interstrand cross-link repair in the Saccharomyces cerevisiae cell cycle: overlapping roles for PSO2 (SNM1) with MutS factors and EXO1 during S phase. Mol. Cell. Biol. 25: 2297–2309.

Castel, A. L., J. D. Cleary, and C. E. Pearson, 2010 Repeat instability as the basis for human diseases and as a potential target for therapy. Nat. Rev. Mol. Cell Biol. 11: 165–170.

Concannon, C., and R. S. Lahue, 2014 Nucleotide excision repair and the 26S proteasome function together to promote trinucleotide repeat expansions. DNA Repair 13: 42–49.

Debacker, K., A. Frizzell, O. Gleeson, L. Kirkham-McCarthy, T. Mertz *et al.*, 2012 Histone deacetylase complexes promote trinucleotide repeat expansions. PLoS Biol. 10: e1001257.

Dixon, M., S. Bhattacharyya, and R. Lahue, 2004 Genetic assays for triplet repeat instability in yeast, pp. 29–45 in *Trinucleotide Repeat Protocols*, edited by Y. Kohwi. Humana Press, New York.

Du, J., E. Campau, E. Soragni, C. Jespersen, and J. M. Gottesfeld, 2013 Length-dependent *CTG·CAG* triplet-repeat expansion in myotonic dystrophy patient-derived induced pluripotent stem cells. Hum. Mol. Genet. 22: 5276–5287.

Foiry, L., L. Dong, C. Savouet, L. Hubert, H. Te Riele *et al.*, 2006 Msh3 is a limiting factor in the formation of intergenerational *CTG* expansions in DM1 transgenic mice. Hum. Genet. 119: 520–526.

Foster, P. L., L. C. Judith, and M. Paul, 2006 Methods for determining spontaneous mutation rates, pp. 195–213 in Measuring Biological Responses with Automated Microscopy (Methods in Enzymology Series, Vol. 414). Academic Press, New York.

Foster, P. L., 2006 Methods for determining spontaneous mutation rates, pp.195–213 in DNA Repair, Part B (Methods in Enzymology Series, Vol. 409). Editors, J.L. Campbell and P. Modrich. Academic Press, New York.

Gacy, A. M., and C. T. McMurray, 1998 Influence of hairpins on template reannealing at trinucleotide repeat duplexes: a model for slipped DNA. Biochemistry 37: 9426–9434.

Gannon, A.-M. M., A. Frizzell, E. Healy, and R. S. Lahue, 2012 MutSβ and histone deacetylase complexes promote expansions of trinucleotide repeats in human cells. Nucleic Acids Res. 40: 10324–10333.

Gietz, D., A. S. Jean, R. A. Woods, and R. H. Schiestl, 1992 Improved method for high efficiency transformation of intact yeast cells. Nucleic Acids Res. 20: 1425.

Goldstein, A. L., and J. H. McCusker, 1999 Three new dominant drug resistance cassettes for gene disruption in Saccharomyces cerevisiae. Yeast 15: 1541–1553.

Gomes-Pereira, M., M. T. Fortune, L. Ingram, J. P. McAbney, and D. G. Monckton, 2004 Pms2 is a genetic enhancer of trinucleotide *CAG·CTG* repeat somatic mosaicism: implications for the mechanism of triplet repeat expansion. Hum. Mol. Genet. 13: 1815–1825.

Halabi, A., S. Ditch, J. Wang, and E. Grabczyk, 2012 DNA mismatch repair complex MutSβ promotes GAA·TTC repeat expansion in human cells. J. Biol. Chem. 287: 29958–29967.

Higham, C. F., and D. G. Monckton, 2013 Modelling and inference reveal nonlinear length-dependent suppression of somatic instability for small disease associated alleles in myotonic dystrophy type 1 and Huntington disease. J. R. Soc. Interface 10: 20130605.

Higham, C. F., F. Morales, C. A. Cobbold, D. T. Haydon, and D. G. Monckton, 2012 High levels of somatic DNA diversity at the myotonic dystrophy type 1 locus are driven by ultra-frequent expansion and contraction mutations. Hum. Mol. Genet. 21: 2450–2463.

Kantartzis, A., G. M. Williams, L. Balakrishnan, R. L. Roberts, J. A. Surtees *et al.*, 2012 Msh2-Msh3 interferes with Okazaki fragment processing to promote trinucleotide repeat expansions. Cell Rep. 2: 216–222.

Kovalenko, M., E. Dragileva, J. St. Claire, T. Gillis, J. R. Guide *et al.*, 2012 Msh2 acts in medium-spiny striatal neurons as an enhancer of CAG instability and mutant huntingtin phenotypes in Huntington's disease knock-in mice. PLoS ONE 7: e44273.

Kumar, C., R. Eichmiller, B. Wang, G. M. Williams, P. R. Bianco *et al.*, 2014 ATP binding and hydrolysis by Saccharomyces cerevisiae Msh2-Msh3 are differentially modulated by mismatch and double-strand break repair DNA substrates. DNA Repair 18: 18–30.

Kumar, C., G. M. Williams, B. Havens, M. K. Dinicola, and J. A. Surtees, 2013 Distinct requirements within the Msh3 nucleotide binding pocket for mismatch and double-strand break repair. J. Mol. Biol. 425: 1881–1898.

Lang, W. H., J. E. Coats, J. Majka, G. L. Hura, Y. Lin *et al.*, 2011 Conformational trapping of mismatch recognition complex MSH2/MSH3 on repair-resistant DNA loops. Proc. Natl. Acad. Sci. USA 108: E837–844.

Lee, J.-M., R. M. Pinto, T. Gillis, J. C. St. Claire, and V. C. Wheeler, 2011 Quantification of age-dependent somatic *CAG* repeat instability in *Hdh CAG* knock-in mice reveals different expansion dynamics in striatum and liver. PLoS ONE 6: e23647.

Leeflang, E. P., S. Tavaré, P. Marjoram, C. O. S. Neal, J. Srinidhi *et al.*, 1999 Analysis of germline mutation spectra at the Huntington's disease locus supports a mitotic mutation mechanism. Hum. Mol. Genet. 8: 173–183.

Leeflang, E. P., L. Zhang, S. Tavare, R. Hubert, J. Srinidhi *et al.*, 1995 Single sperm analysis of the trinucleotide repeats in the Huntington's disease gene: quantification of the mutation frequency spectrum. Hum. Mol. Genet. 4: 1519–1526.

Li, G.-M., 2008 Mechanisms and functions of DNA mismatch repair. Cell Res. 18: 85–98.

Lovett, S. T., 2004 Encoded errors: mutations and rearrangements mediated by misalignment at repetitive DNA sequences. Mol. Microbiol. 52: 1243–1253.

Lyndaker, A. M., T. Goldfarb, and E. Alani, 2008 Mutants defective in Rad1-Rad10-Slx4 exhibit a unique pattern of viability during mating-type switching in *Saccharomyces cerevisiae*. Genetics 179: 1807–1821.

Manley, K., J. Pugh, and A. Messer, 1999 Instability of the *CAG* repeat in immortalized fibroblast cell cultures from Huntington's disease transgenic mice. Brain Res. 835: 74–79.

Marquis Gacy, A., G. Goellner, N. Juranic, S. Macura, and C. T. McMurray, 1995 Trinucleotide repeats that expand in human disease form hairpin structures in vitro. Cell 81: 533–540.

Martorell, L., J. Gámez, M. L. Cayuela, F. K. Gould, J. P. McAbney *et al.*, 2004 Germline mutational dynamics in myotonic dystrophy type 1 males: allele length and age effects. Neurology 62: 269–274.

Maurer, D. J., B. L. O'Callaghan, and D. M. Livingston, 1996 Orientation dependence of trinucleotide *CAG* repeat instability in Saccharomyces cerevisiae. Mol. Cell. Biol. 16: 6617–6622.

McMurray, C. T., 2010 Mechanisms of trinucleotide repeat instability during human development. Nat. Rev. Genet. 11: 786–799.

Miret, J. J., L. Pessoa-Brandão, and R. S. Lahue, 1997 Instability of *CAG* and *CTG* trinucleotide repeats in Saccharomyces cerevisiae. Mol. Cell. Biol. 17: 3382–3387.

Miret, J. J., L. Pessoa-Brandão, and R. S. Lahue, 1998 Orientation-dependent and sequence-specific expansions of *CTG/CAG* trinucleotide repeats in Saccharomyces cerevisiae. Proc. Natl. Acad. Sci. USA 95: 12438–12443.

Morales, F., J. M. Couto, C. F. Higham, G. Hogg, P. Cuenca *et al.*, 2012 Somatic instability of the expanded *CTG* triplet repeat in myotonic dystrophy type 1 is a heritable quantitative trait and modifier of disease severity. Hum. Mol. Genet. 21: 3558–3567.

Owen, B. A., W. H. Lang, and C. T. McMurray, 2009 The nucleotide binding dynamics of human MSH2-MSH3 are lesion dependent. Nat. Struct. Mol. Biol. 16: 550–557.

Owen, B. A., Z. Yang, M. Lai, M. Gajec, J. d. Badger *et al.*, 2005 $(CAG)_n$-hairpin DNA binds to Msh2-Msh3 and changes properties of mismatch recognition. Nat. Struct. Mol. Biol. 12: 663–670.

Panigrahi, G. B., R. Lau, S. E. Montgomery, M. R. Leonard, and C. E. Pearson, 2005 Slipped (*CTG*)·(*CAG*) repeats can be correctly repaired, escape repair or undergo error-prone repair. Nat. Struct. Mol. Biol. 12: 654–662.

Panigrahi, G. B., M. M. Slean, J. P. Simard, O. Gileadi, and C. E. Pearson, 2006 Isolated short *CTG/CAG* DNA slip-outs are repaired efficiently by hMutSβ, but clustered slip-outs are poorly repaired. Proc. Natl. Acad. Sci. USA 107: 12593–12598.

Park, J. M., S. Huang, D. Tougeron, and F. A. Sinicrope, 2013 MSH3 mismatch repair protein regulates sensitivity to cytotoxic drugs and a histone deacetylase inhibitor in human colon carcinoma cells. PLoS ONE 8: e65369.

Pearson, C. E., and R. R. Sinden, 1996 Alternative structures in duplex DNA formed within the trinucleotide repeats of the myotonic dystrophy and fragile X loci. Biochemistry 35: 5041–5053.

Pearson, C. E., and R. R. Sinden, 1998 Trinucleotide repeat DNA structures: dynamic mutations from dynamic DNA. Curr. Opin. Struct. Biol. 8: 321–330.

Pinto, R. M., E. Dragileva, A. Kirby, A. Lloret, E. Lopez *et al.*, 2013 Mismatch repair genes *Mlh1* and *Mlh3* modify *CAG* instability in Huntington's disease mice: genome-wide and candidate approaches. PLoS Genet. 9: e1003930.

Pluciennik, A., V. Burdett, C. Baitinger, R. R. Iyer, K. Shi *et al.*, 2013 Extrahelical (*CAG*)/(*CTG*) triplet repeat elements support proliferating cell nuclear antigen loading and MutLα endonuclease activation. Proc. Natl. Acad. Sci. USA 110: 12277–12282.

Rogacheva, M. V., C. M. Manhart, C. Chen, A. Guarne, J. Surtees *et al.*, 2014 Mlh1-Mlh3, a meiotic crossover and DNA mismatch repair factor, is a Msh2-Msh3-stimulated endonuclease. J. Biol. Chem. 289: 5664–5673.

Rolfsmeier, M. L., M. J. Dixon, L. Pessoa-Brandão, R. Pelletier, J. J. Miret *et al.*, 2001 *Cis*-elements governing trinucleotide repeat instability in *Saccharomyces cerevisiae*. Genetics 157: 1569–1579.

Romanova, N. V., and G. F. Crouse, 2013 Different roles of eukaryotic MutS and MutL complexes in repair of small insertion and deletion loops in yeast. PLoS Genet. 9: e1003920.

Sambrook, J., and D. W. Russell, 2001 *Molecular Cloning: A Laboratory Manual*, Ed. 3rd. Cold Spring Harbor Laboratory Press, Cold Spring Harbor, NY.

Schweitzer, J. K., and D. M. Livingston, 1997 Destabilization of *CAG* trinucleotide repeat tracts by mismatch repair mutations in yeast. Hum. Mol. Genet. 6: 349–355.

Sia, E., R. Kokoska, M. Dominska, P. Greenwell, and T. Petes, 1997 Microsatellite instability in yeast: dependence on repeat unit size and DNA mismatch repair genes. Mol. Cell. Biol. 17: 2851–2858.

Slean, M. M., K. Reddy, B. Wu, K. Nichol Edamura, M. Kekis *et al.*, 2013 Interconverting conformations of slipped-DNA junctions formed by trinucleotide repeats affect repair outcome. Biochemistry 52: 773–785.

Stevens, J. R., E. E. Lahue, G.-M. Li, and R. S. Lahue, 2013 Trinucleotide repeat expansions catalyzed by human cell-free extracts. Cell Res. 23: 565–572.

Surtees, J. A., J. L. Argueso, and E. Alani, 2004 Mismatch repair proteins: key regulators of genetic recombination. Cytogenet. Genome Res. 107: 146–159.

Takahashi, M., M. Koi, F. Balaguer, C. R. Boland, and A. Goel, 2011 MSH_3 mediates sensitization of colorectal cancer cells to cisplatin, oxaliplatin, and a poly(ADP-ribose) polymerase inhibitor. J. Biol. Chem. 286: 12157–12165.

Tomé, S., K. Manley, J. P. Simard, G. W. Clark, M. M. Slean *et al.*, 2013 MSH3 polymorphisms and protein levels affect CAG repeat instability in Huntington's disease mice. PLoS Genet. 9: e1003280.

van den Broek, W. J. A. A., M. R. Nelen, D. G. Wansink, M. M. Coerwinkel, H. te Riele *et al.*, 2002 Somatic expansion behaviour of the $(CTG)_n$ repeat in myotonic dystrophy knock-in mice is differentially affected by Msh3 and Msh6 mismatch-repair proteins. Hum. Mol. Genet. 11: 191–198.

van Oers, J. M. M., Y. Edwards, R. Chahwan, W. Zhang, C. Smith *et al.*, 2013 The MutSβ complex is a modulator of p53-driven tumorigenesis through its functions in both DNA double-strand break repair and mismatch repair. Oncogene 33: 3939–3946.

Wach, A., A. Brachat, R. Pohlmann, and P. O. Philippsen, 1994 New heterologous modules for classical or PCR-based gene disruptions in Saccharomyces cerevisiae. Yeast 10: 1793–1808.

Zar, J. H., 1999 *Biostatistical Analysis*, Ed. 4th. Prentice Hall, Upper Saddle River, NJ.

Zhang, L., E. P. Leeflang, J. Yu, and N. Arnheim, 1994 Studying human mutations by sperm typing: instability of *CAG* trinucleotide repeats in the human androgen receptor gene. Nat. Genet. 7: 531–535.

Zhao, J., A. Jain, R. R. Iyer, P. L. Modrich, and K. M. Vasquez, 2009 Mismatch repair and nucleotide excision repair proteins cooperate in the recognition of DNA interstrand cross-links. Nucleic Acids Res. 37: 4420–4429.

Communicating editor: J. A. Nickoloff

GENETICS

Supporting Information
www.genetics.org/lookup/suppl/doi:10.1534/genetics.115.177303/-/DC1

MSH3 Promotes Dynamic Behavior of Trinucleotide Repeat Tracts *In Vivo*

Gregory M. Williams and Jennifer A. Surtees

DOI: 10.1534/genetics.115.177303

Table S1. Background stains used to integrate TNR tracts.

Strain No.	Genotype	Derived from strain	Source
FY86	*MAT*a *ura3-52 leu2Δ1 his3Δ200*		Winston, 1995
JSY1501	*MAT*a *ura3-52 leu2Δ1 his3Δ200 msh3Δ::KANMX*	FY86	Kantartzis, 2012
JSY1515	*MAT*a *ura3-52 leu2Δ1 his3Δ200 msh3Δ::hisG*	FY86	This study

Table S2. Initial expansion size of trinucleotide repeat tracts[a]

Genotype	Tract sequence	Median size (net change)[b]	Range (net change)[b]
MSH3 (n=61)	*CAG*	42 (+17)	31-67 (+6 to +42)
MSH3 (n=89)	*CTG*	33 (+8)	26-43 (+1 to +18)
msh3Δ (n=38)	*CAG*	31 (+6)	31-48 (+6 to +16)
msh3Δ (n=35)	*CTG*	33.5 (+8)	28-39 (+3 to +14)

[a] Initial expansion sizes obtained from all time course experiments.

[b] Number of repeats in TNR tract

Supplementary Figures

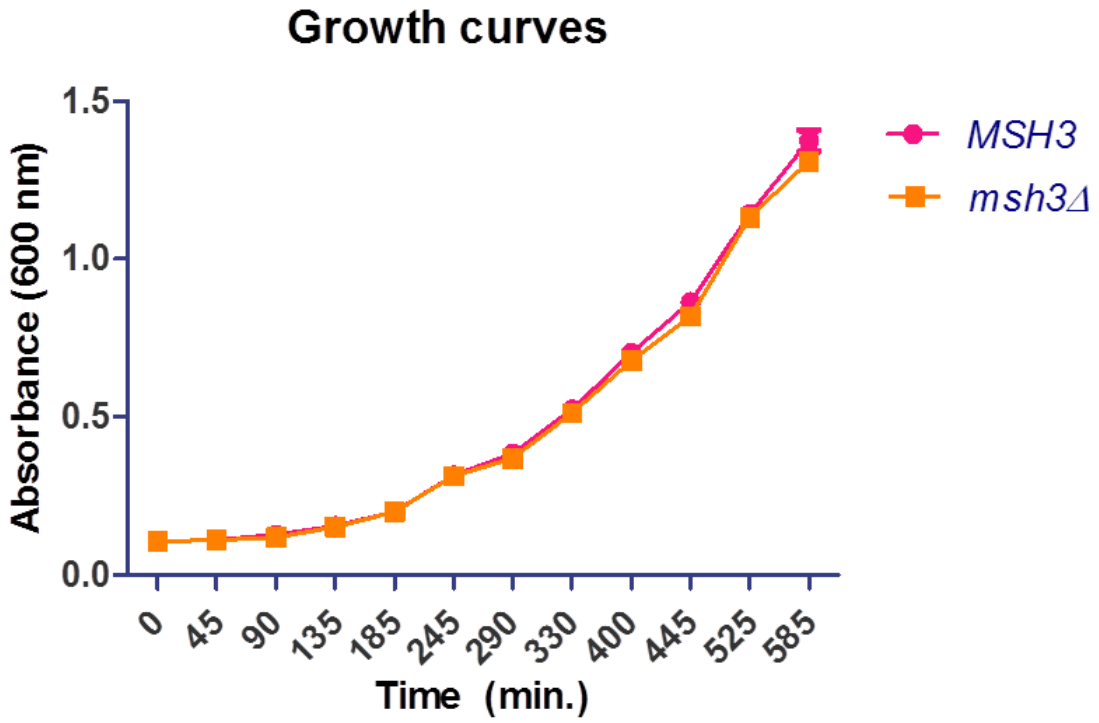

Figure S1. Growth curves of *MSH3* and *msh3Δ* strains. Growth curve experiments were performed with two independent isolates each of *MSH3(CTG)*$_{25}$ and *MSH3(CAG)*$_{25}$, in parallel, measuring absorbance (600 nm) as a function of time. These curves were averaged and the standard error of the mean (S.E.M.) calculated for each time point (pink circles). Similarly, growth curve experiments were performed with two independent isolates each of *msh3Δ(CTG)*$_{25}$ and *msh3Δ(CAG)*$_{25}$ (orange squares).

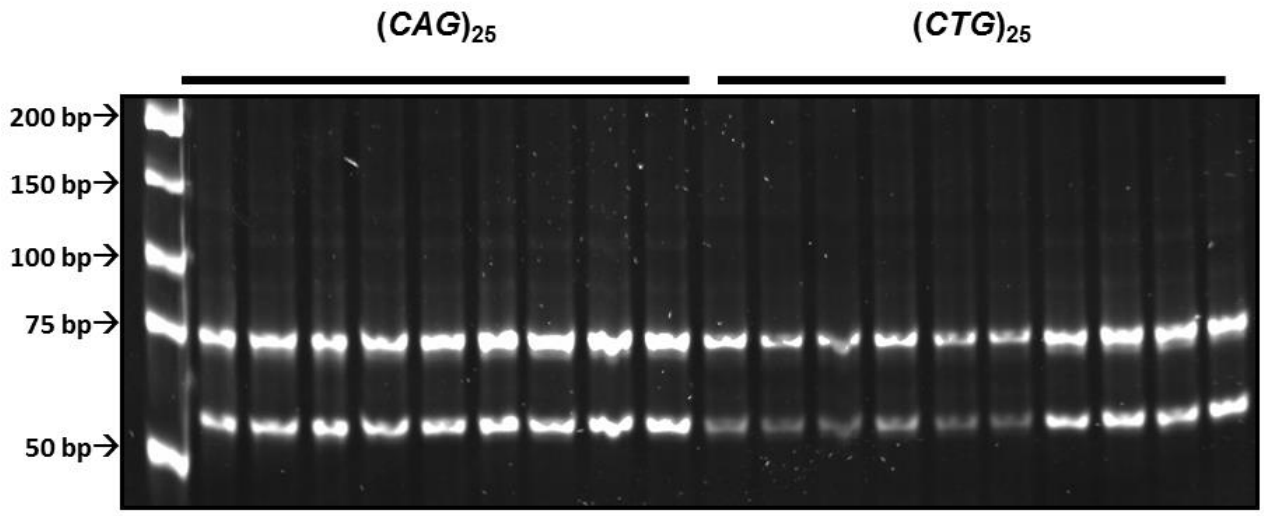

Figure S2. Control PCR reactions to amplify unexpanded TNR tract from plasmid.
Nineteen independent PCR amplification of the TNR tract from pBL170 $(CAG)_{25}$ and pBL169 $(CTG)_{25}$ (Miret *et al.*, 1998) separated by native gel electrophoresis on a 12% polyacrylamide gel. The PCR products were digested with *Sph*I and *Afl*II, which releases a product containing only the tract. The lower band is a product of this digestion. The unexpanded tract is 75 bp (25 repeats).

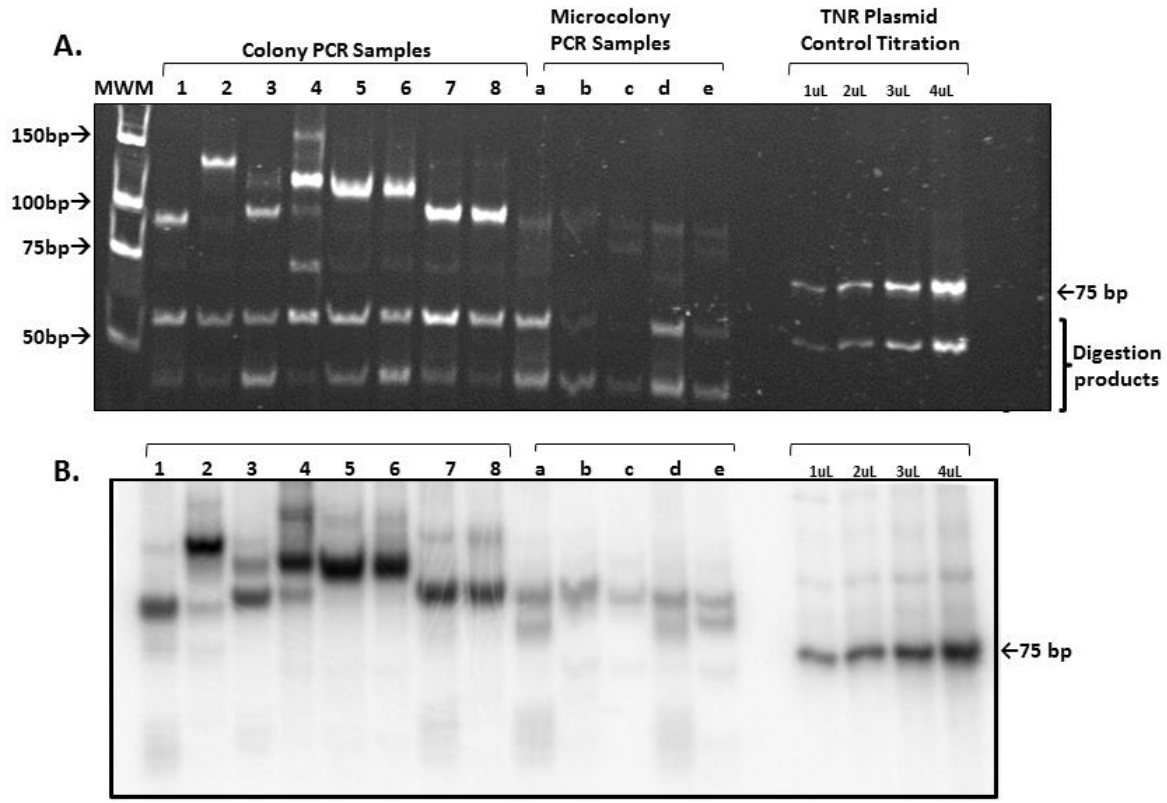

Figure S3. Specificity of probe used for Southern blots. The TNR tract from *MSH3* was amplified by PCR from representative colonies and microcolonies and digested with *Sph*I and *Afl*II to release the TNR tract. **A.** The resulting products were separated on a 12% polyacrylamide gel. A titration of a control reaction using plasmid DNA as a template was electrophoresed alongside these reactions (1μL – 4μL). **B.** The gel in **A** was subjected to Southern blot using a (*CTG*)-containing probe. The TNR probe specifically interacted with TNR-containing fragments, but not other DNA products.

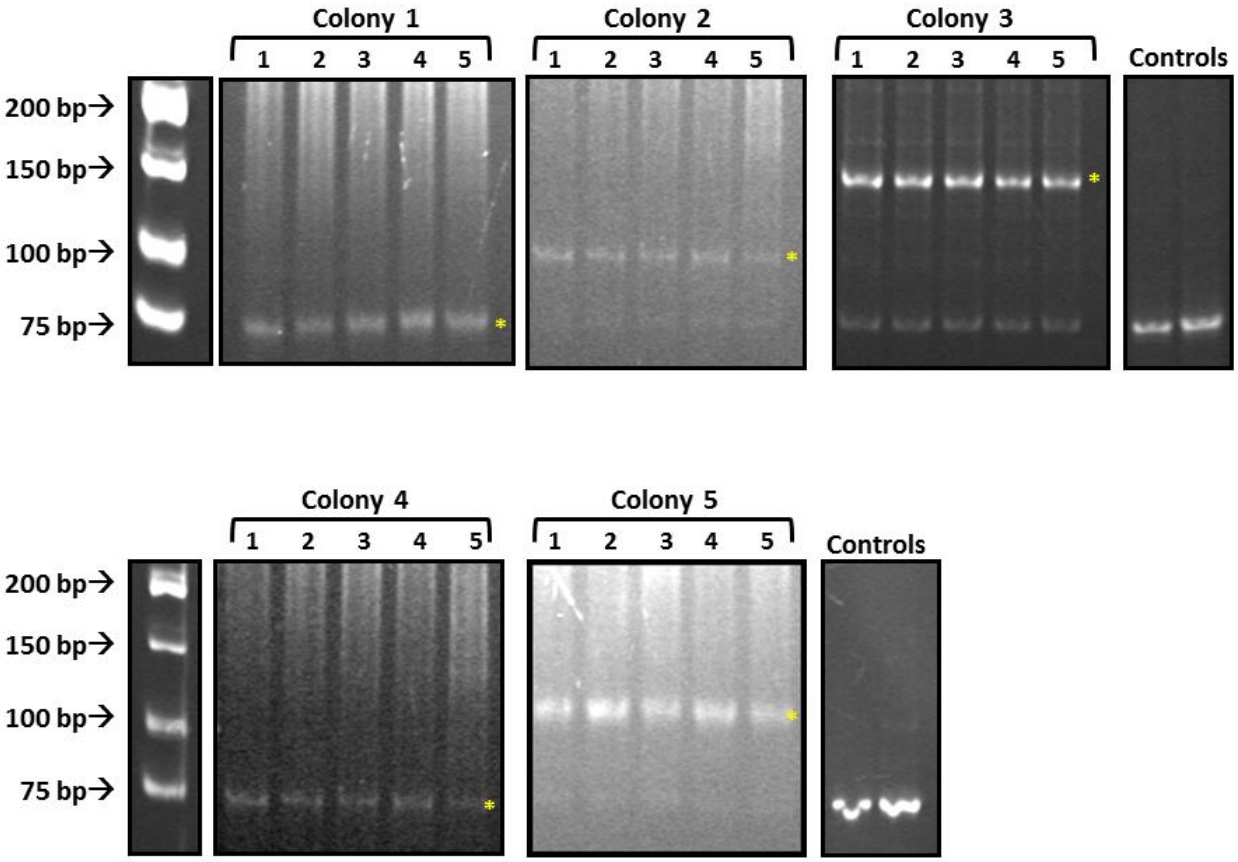

Figure S4. Control colony PCR amplification of unexpanded and expanded TNR tracts. In each panel, five independent PCR reactions were performed in parallel from a single colony selected on 5-FOA to determine reproducibility of these reactions. PCR products were digested with *Sph*I and *Afl*II to release the tract. The other digestion products are not shown. The unexpanded tract is 75 bp.

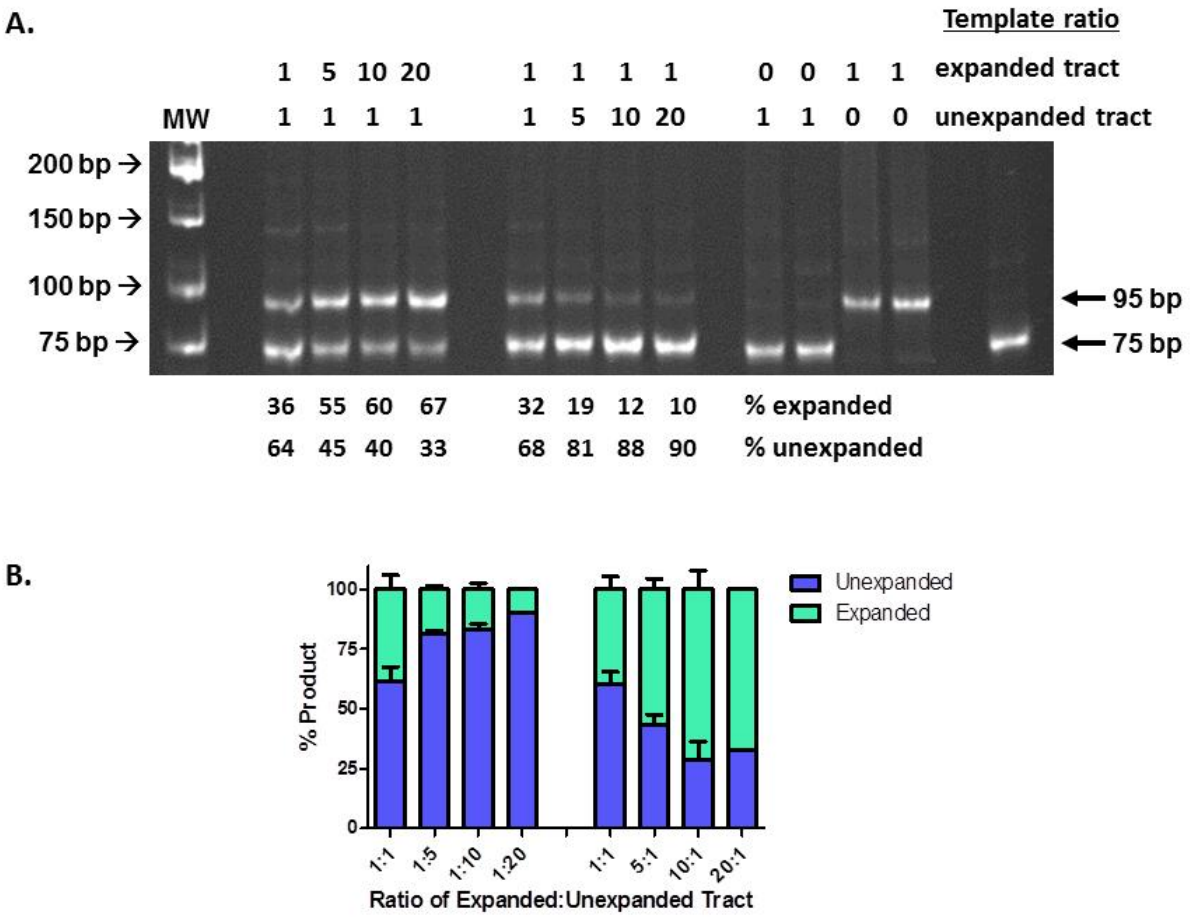

Figure S5. PCR amplification products correlate with input template DNA. A. Different ratios of unexpanded:expanded (1:1, 1:5, 1:10, 1:20) tract (genomic DNA) were used as a substrate for PCR; the total template DNA was constant at 5 μg. The amount of input template correlates with the PCR product output, although there is a small but significant bias toward the unexpanded tract. **B.** The relative amounts of expanded and unexpanded PCR product as a function of input template ratio is plotted. The error bars indicate the S.E.M. of three independent experiments.

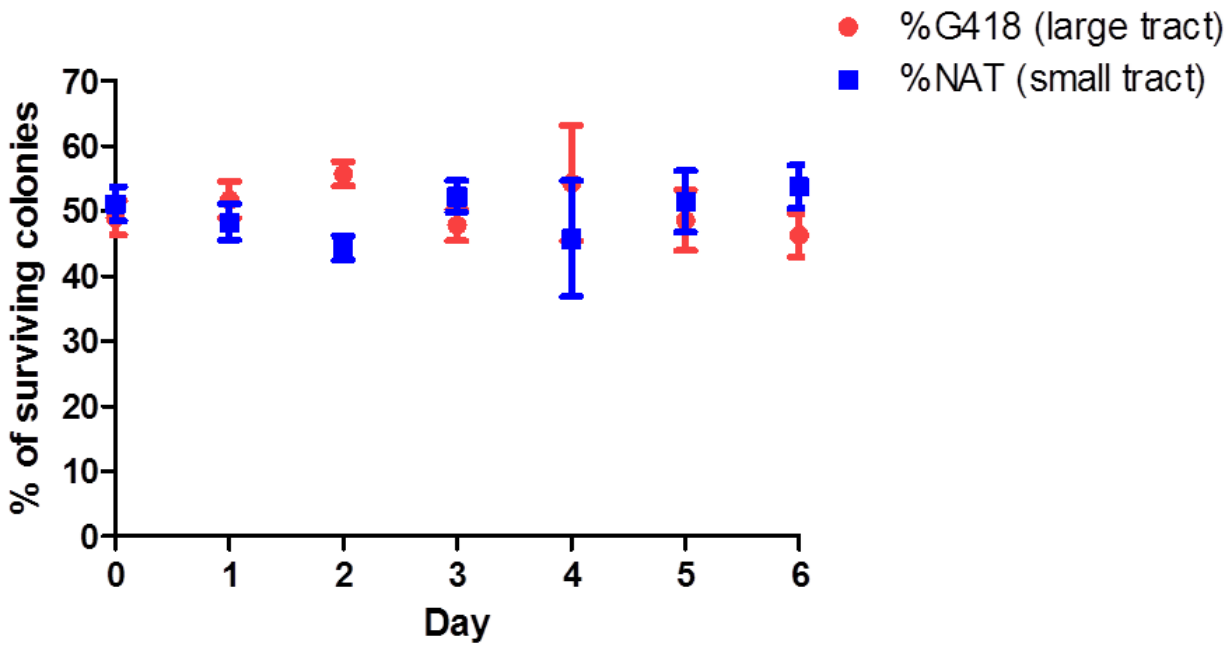

Figure S6. A larger TNR tract does not confer a selective advantage. A *MSH3* strain encoding a large TNR tract (>40 repeats) was transformed with a low copy plasmid encoding the KANMX cassette, conferring resistance to G418. A *MSH3* strain encoding a short (<30 repeats) TNR tract was transformed with a low copy plasmid encoding the NATMX cassette, conferring resistance to clonNAT. These cells were mixed at a 1:1 ratio and the mixture was grown as a log phase culture (see **Fig. S4A**), in the absence of selection, for 6 days. Cells were plated and the percentage that retained either the KANMX (red circles) or the NATMX (blue squares) cassette was determined. An average of three independent experiments (± SEM) is shown.

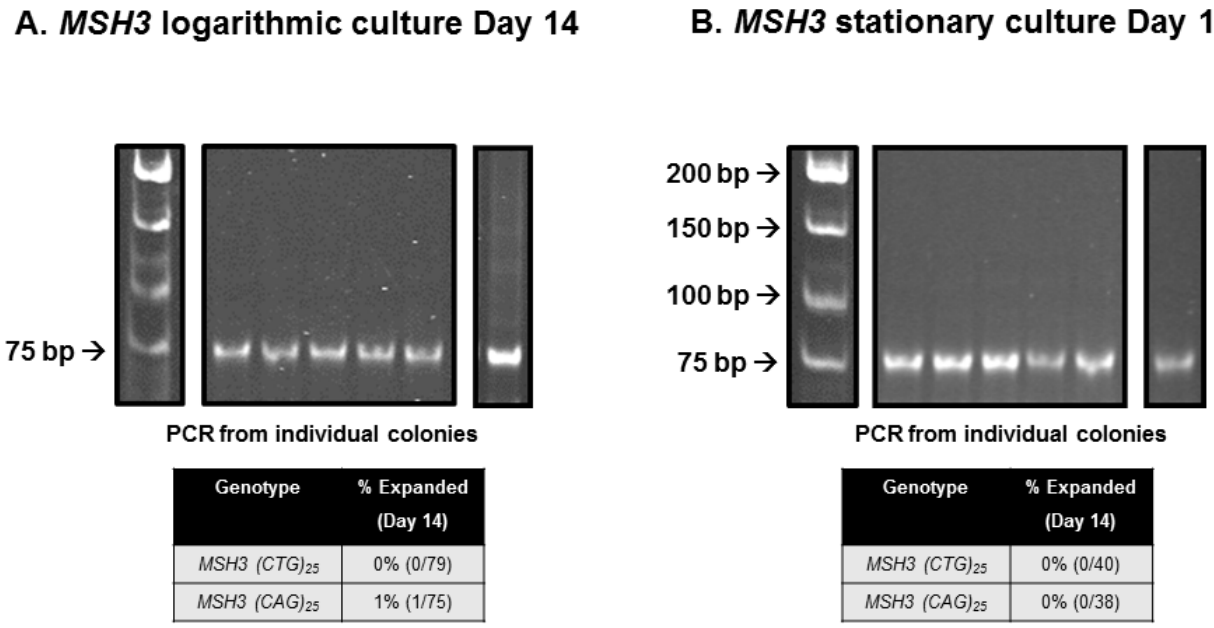

Genotype	% Expanded (Day 14)
MSH3 $(CTG)_{25}$	0% (0/79)
MSH3 $(CAG)_{25}$	1% (1/75)

Genotype	% Expanded (Day 14)
MSH3 $(CTG)_{25}$	0% (0/40)
MSH3 $(CAG)_{25}$	0% (0/38)

Figure S7. Liquid time course experiments in *MSH3(CTG)$_{25}$* and *MSH3(CAG)$_{25}$* logarithmic and stationary cultures to determine population tract dynamics. We performed time course experiments with *MSH3* strains containing *unexpanded CTG* and *CAG* tracts in **A.** logarithmic and **B.** stationary phase cultures. Tract sizes were confirmed by PCR prior to starting the experiment. **Top panel:** Samples from Day 14 cultures were plated on minimal media lacking histidine to obtain individual colonies. Colony PCR was performed to amplify the TNR tract from colonies to determine individual tract lengths within the population. The arrows indicate tracts that have incurred an additional expansion. The number below

each tract indicates the number of repeats within each tract. Control PCR reactions using the TNR plasmid (C) were performed alongside each set as a marker for the 75 base pair (bp) tract (25 repeats). Summary of expansion frequency at Day 14 in the different genetic backgrounds tested, based on PCR amplification of tracts from individual colonies. Mutation rates from these data were calculated and are shown in **Table 1**.

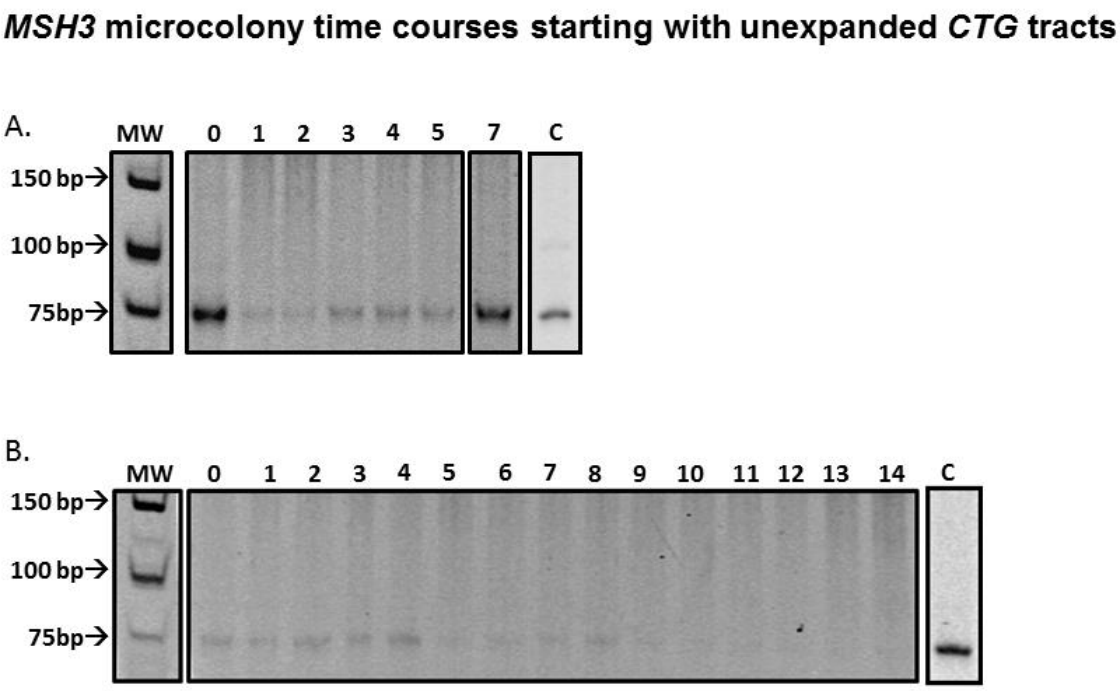

Figure S8. Unexpanded TNR tracts are stable starting from a single cell. Two examples of microcolony time courses starting with *unexpanded* tracts in a *MSH3* $(CTG)_{25}$ background. Tract sizes were confirmed by PCR. Individual cells from these colonies were isolated and allowed to undergo 8-10 rounds of replication, resulting in a microcolony approximately 250-1000 cells in size. A single cell was then taken from this microcolony to propagate another microcolony. The remainder was used to amplify the TNR tract by PCR to determine tract length (see **Fig. 10** for cartoon). No tract changes were observed. Both gels are 12% polyacrylamide gels stained with EtBr; the images of been inverted for ease of viewing. The lanes marked **C** in each panel indicate the 75bp tract amplified from the TNR plasmid control.

The numbers across the top of the gels indicate the time point. A mutation rate for these experiments was calculated and is shown in **Table 1**.